

Supporting Information for: Optoelectronic Properties of Quadrupolar and Bi-Quadrupolar Dyes: Intra and Inter Chromophoric Interactions

Olatz Uranga-Barandiaran,^{†,‡} Manon Catherin,[¶] Elena Zabrova,[¶] Anthony d'Aléo,[§] Frédéric Fages,^{*,¶} Frédéric Castet,^{*,‡} and David Casanova^{*,||}

[†]*Kimika Fakultatea, Euskal Herriko Unibertsitatea (UPV/EHU), 20018 Donostia, Euskadi, Spain*

[‡]*Institut des Sciences Moléculaires (ISM, UMR CNRS 5255), University of Bordeaux, 351 Cours de la Libération, 33405 Talence, France*

[¶]*Aix-Marseille Univ, CNRS, CINaM UMR 7325, Campus de Luminy, Case 913, 13288 Marseille, France*

[§]*Building Blocks for Future Electronics Laboratory (2-B FUEL), The joint CNRS-Ewha-Yonsei Laboratory, UMI 2002, Seoul, Republic of Korea*

^{||}*Donostia International Physics Center (DIPC), Paseo Manuel de Lardizabal 4, 20018 Donostia, Euskadi, Spain*

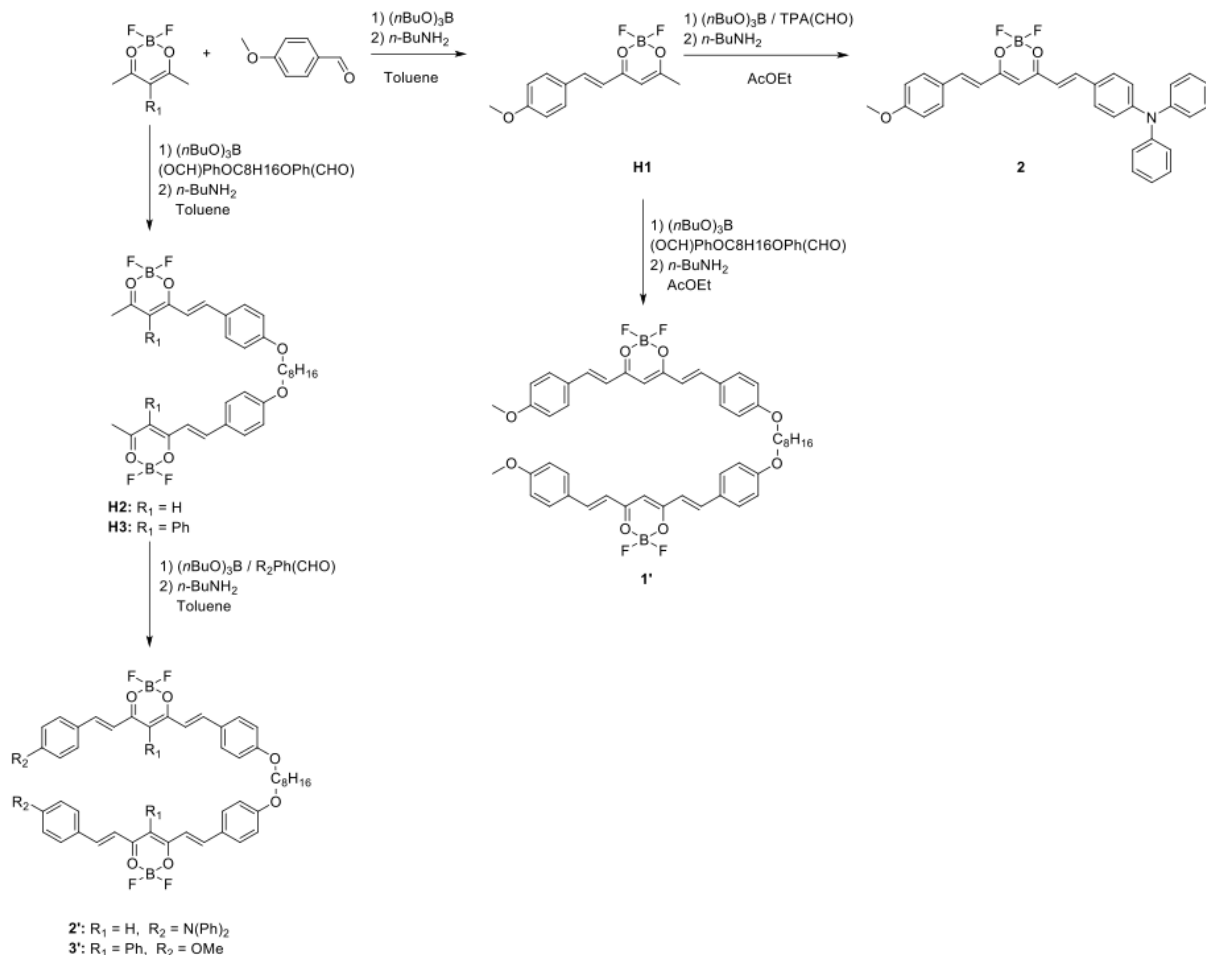
E-mail: frederic.fages@univ-amu.fr; frederic.castet@u-bordeaux.fr; david.casanova@ehu.eus

Contents

1 Synthesis of the curcumin derivatives	3
1.1 Difluoro(3-phenylpentane-2,4-dionato)boron ²	4
1.2 BF ₂ -hemicurcuminoid H1 ³	5
1.3 Bis(BF ₂ -hemicurcuminoid)- α , ω -octane H2	7
1.4 BF ₂ -hemicurcuminoid H3	9
1.5 Monomer 2	11
1.6 Dimer 1	13
1.7 Dimer 2	14
1.8 Absorption spectra of monomers 1 and 2 in different solvents	16
2 Excitation energies: functional and basis set	17
2.1 Curcumin monomers	17
2.2 Curcumin derivative dimers	19
3 Rotation of the <i>meso</i>-phenyl in monomer 3	23
4 Relative energies between open/folded conformers	24
5 Absorption spectra: vibronic resolution	25
6 Diabatization of low-lying states	25
6.1 Diabatization scheme: Edmiston-Ruedenberg localization	25
6.2 Decomposition in the diabatic basis: dimers	26
6.3 Electronic Hamiltonians	27
6.3.1 Electronic Hamiltonians of curcumin monomers	27
6.3.2 Electronic Hamiltonians of curcumin dimers	28
7 Fragment charge distribution	29
7.1 Curcumin derivatives: monomers	29
7.2 Curcumin derivatives: dimers	30
8 Splitting of S₁ and S₂ in dimer 2'	32
9 Dimer 2': CAM-B3LYP calculations	33
References	34

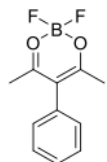
1 Synthesis of the curcumin derivatives

All solvents for synthesis were of analytic grade. NMR spectra were recorded at room temperature on a JEOL JNM ECR 400 (400 and 100 MHz for ^1H and ^{13}C , respectively) spectrometer. Data are listed in parts per million (ppm) and are reported relative to tetramethylsilane (^1H and ^{13}C); residual solvent peaks of the deuterated solvents were used as internal standards. High resolution mass spectra were obtained in Spectropole, Marseille (<http://www.spectropole.fr>). 1,8-Bis(4-formylphenoxy)octane was obtained according a previously described procedure.¹ All starting chemical products and solvents were purchased from Sigma-Aldrich or TCI and used without further purification.

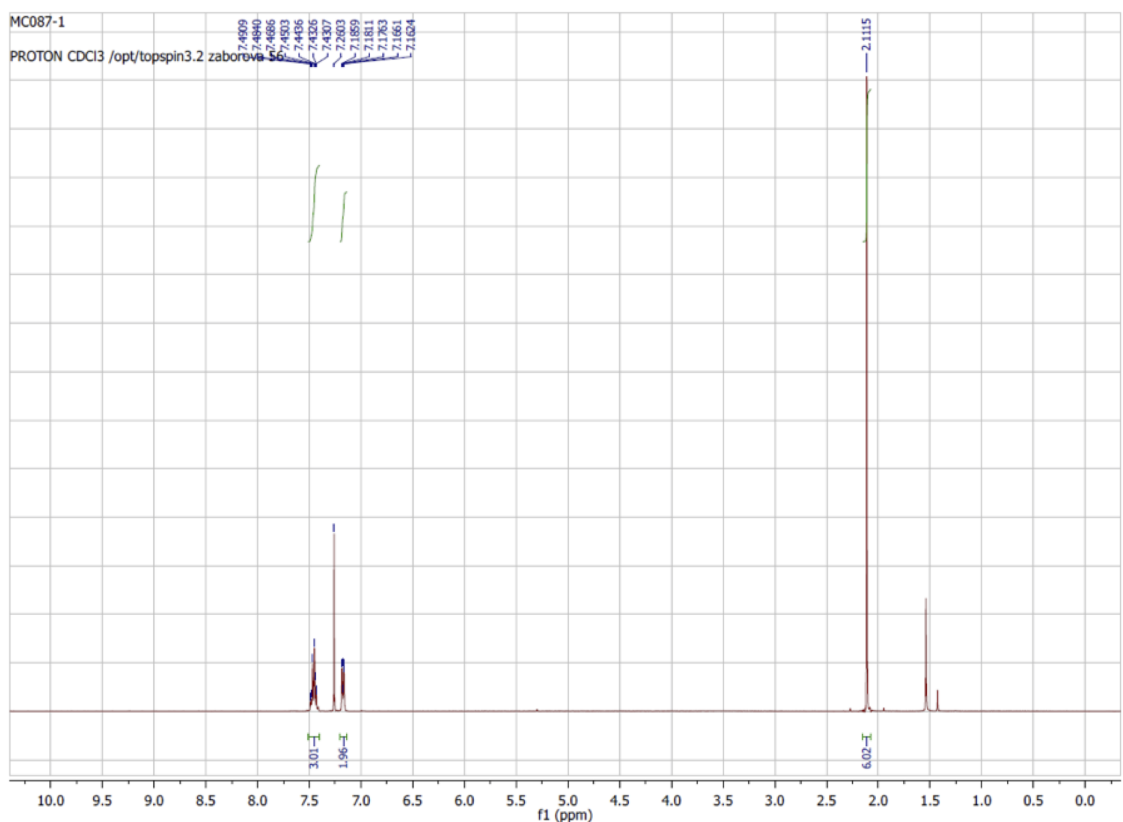


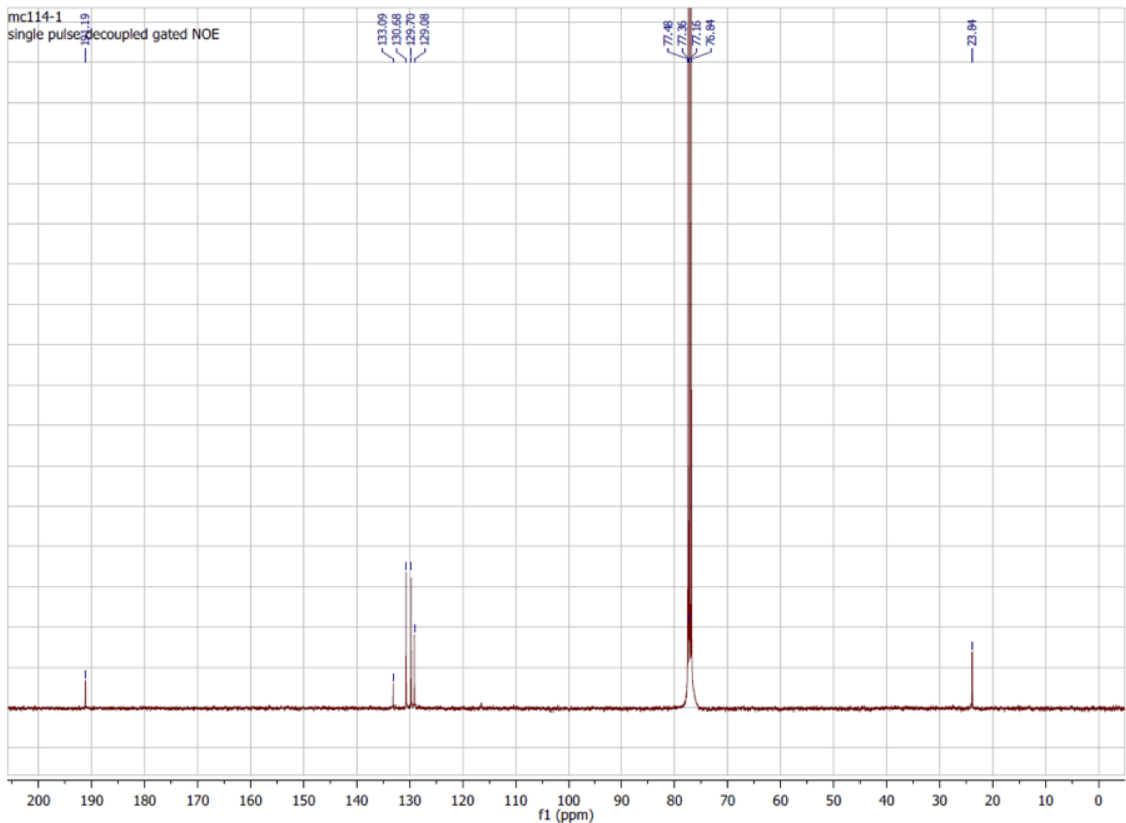
Scheme S1

1.1 Difluoro(3-phenylpentane-2,4-dionato)boron²

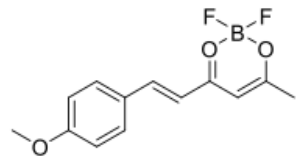


Boron trifluoride diethyletherate (3.51 mL, 27.92 mmol) was added dropwise to a solution of 3-phenylpentane-2,4-dione (4.1 g, 23.27 mmol) in dichloromethane (100 mL). The reaction mixture was stirred at 40 °C overnight. After cooling, solvents were removed under vacuum and the crude was purified on silica gel column with dichloromethane/cyclohexane (1/1 v:v) as eluent. The result product was obtained as a white solid (5.01 g, 96 %). ¹H NMR (400 MHz, CDCl₃, ppm): δ = 7.50 – 7.40 (m, 3H), 7.20 – 7.14 (m, 2H), 2.11 (s, 6H). ¹³C NMR (100 MHz, CDCl₃, ppm): δ = 191.2, 133.1, 130.7, 129.7, 129.1, 23.8.



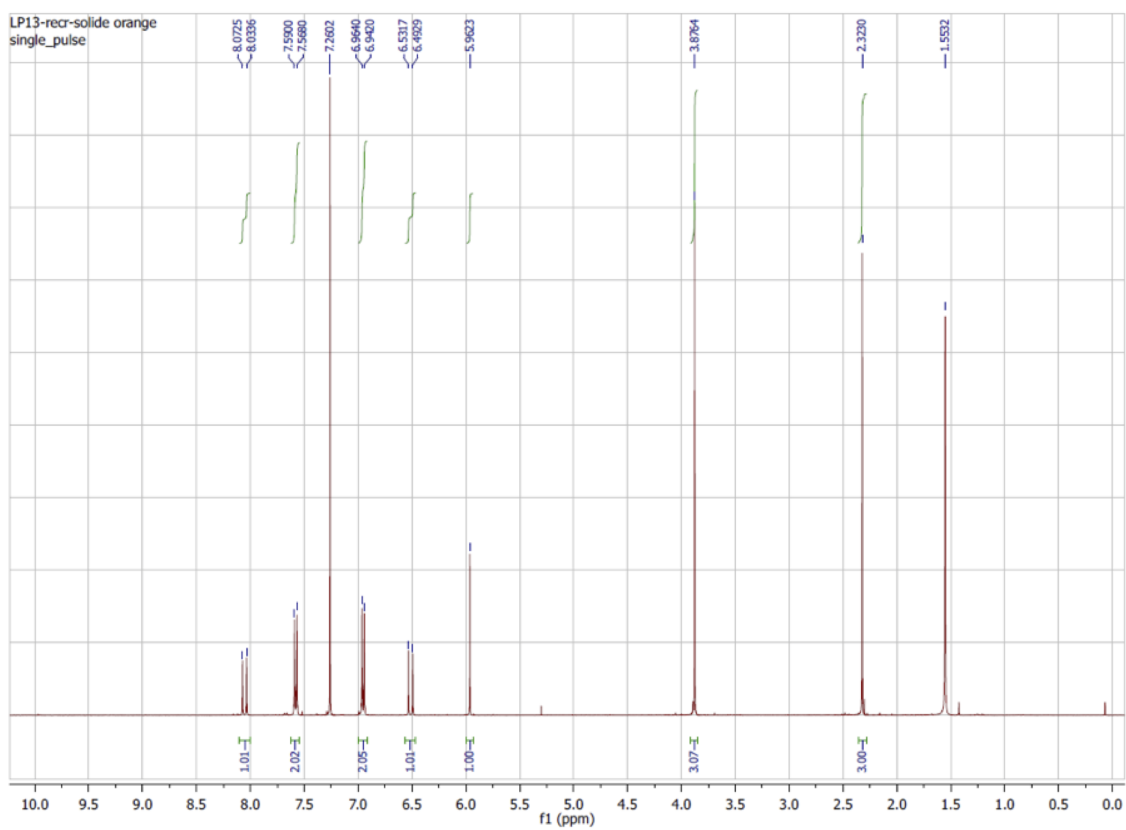


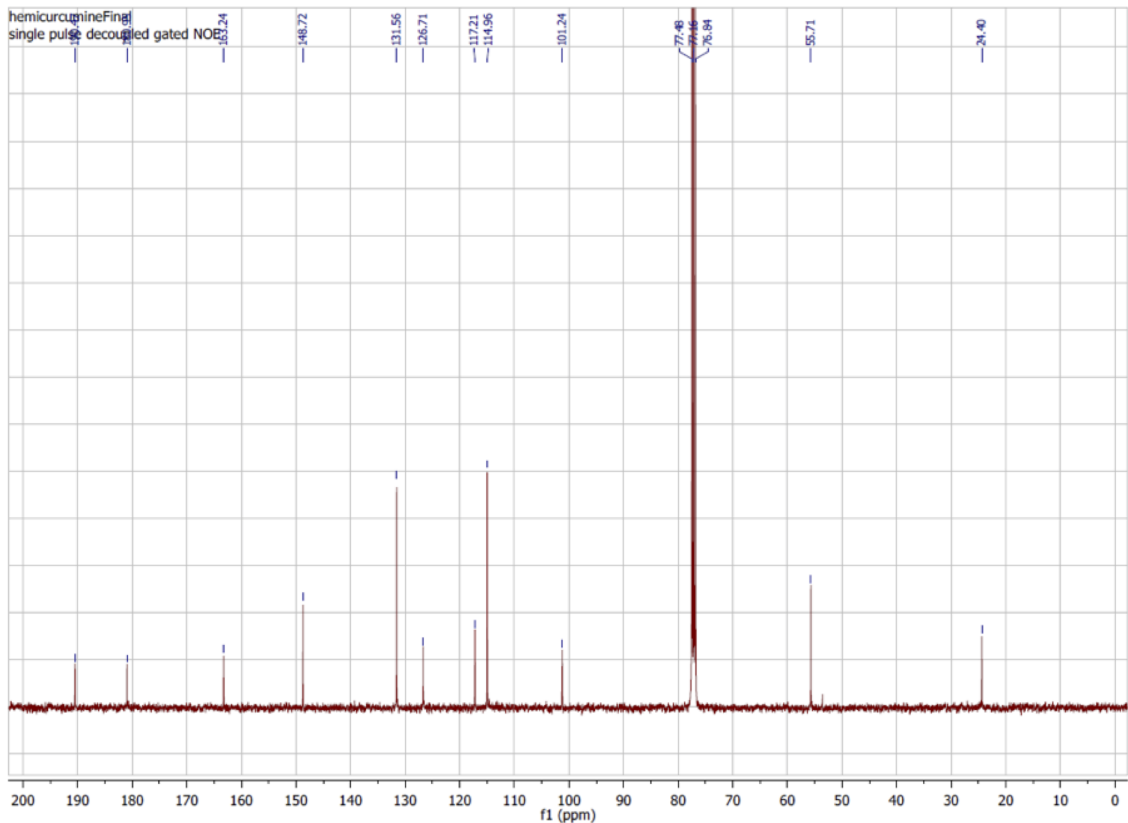
1.2 BF_2 -hemicurcuminoid H1³



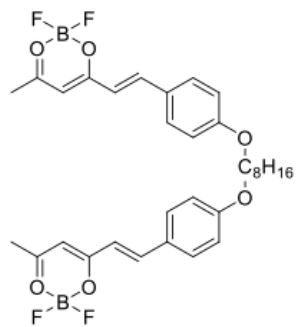
(Acetylacetonato)difluoroboron (5.38 g, 36.40 mmol) was dissolved into 100 mL of toluene and stirred at reflux for 30 min under argon. Then a solution of p-anisaldehyde (1.11 mL, 9.10 mmol) and tri-*n*-butylborate (2.71 mL, 10.01 mmol) in 100 mL of toluene was added dropwise and the reaction mixture was stirred for 30 min under reflux. A first portion of *n*-butylamine (450 μL , 4.55 mmol) was added and after 2 h a second portion of *n*-butylamine (450 μL , 4.55 mmol) was added and the reaction mixture was stirred under reflux overnight. Solvent was removed under vacuum and the crude was purified on silica gel column with cyclohexane/dichloromethane (1/1 v:v) as eluent. The product was obtained as a yellow powder (1.47 g, 61 %). ^1H NMR (400 MHz, CDCl_3 , ppm): δ = 8.05 (d, J = 15.5 Hz, 1H), 7.58 (d, J = 8.8 Hz, 2H), 6.96 (d, J = 8.8 Hz, 2H), 6.51 (d, J = 15.5 Hz, 1H), 5.96 (s, 1H),

3.88 (s, 3H), 2.32 (s, 3H). ^{13}C NMR (100 MHz, CDCl_3 , ppm): $\delta = 190.5, 180.9, 163.2, 148.7, 131.6, 126.7, 117.2, 115.0, 101.2, 55.7, 24.4$.



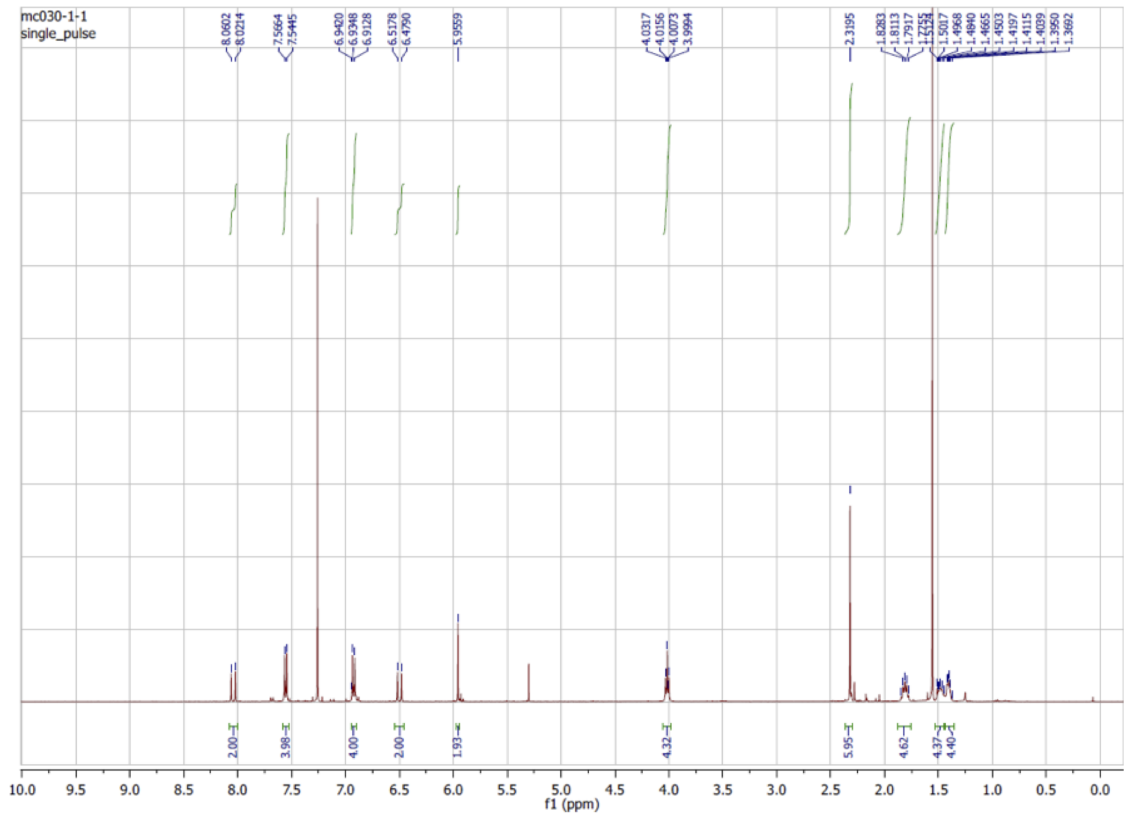


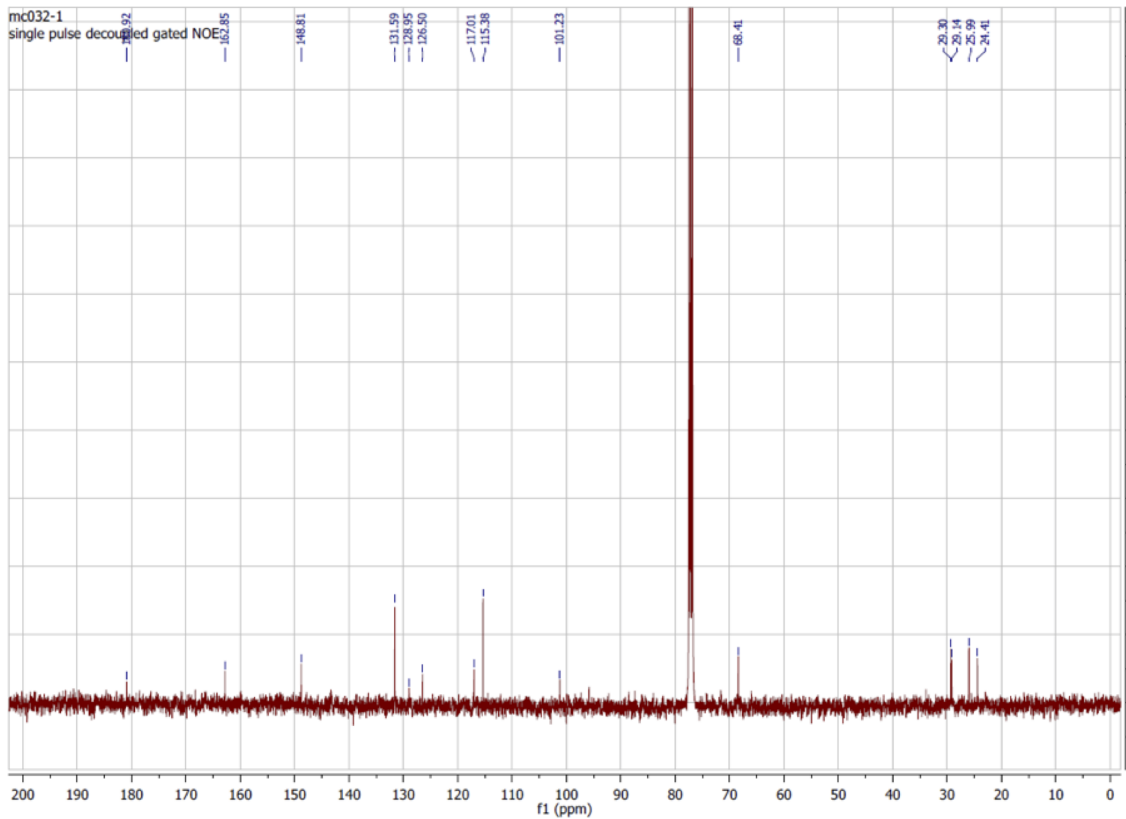
1.3 Bis(BF₂-hemicuminoid)- α,ω -octane H2



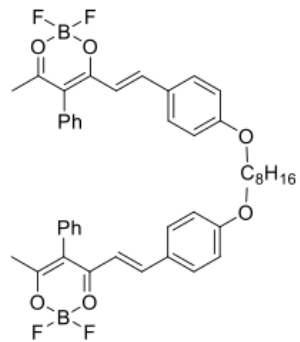
(Acetylacetonato)difluoroboron (3.33 g, 22.56 mmol) was dissolved into 50 mL of toluene and stirred at reflux for 30 min under argon. 1,8-Bis(4-formylphenoxy)octane (1.0 g, 2.82 mmol) and tri-*n*-butylborate (763 μ L, 2.82 mmol) were dissolved into 100 mL of toluene and the solution was added dropwise to the reaction mixture. After stirring for 30 min at reflux, a first portion of *n*-butylamine (139 μ L, 1.41 mmol) was added. A second portion of *n*-butylamine (139 μ L, 1.41 mmol) was added after 3h and the reaction mixture was stirred at reflux

overnight. After cooling, the reaction mixture was filtered and the solvent was removed under vacuum. The crude was purified on silica gel column with dichloromethane/cyclohexane (1/1 v:v) as eluent. The product was obtained as an orange powder (601 mg, 35 %). ^1H NMR (400 MHz, CDCl_3 , ppm): $\delta = 8.04$ (d, $J = 15.5$ Hz, 2H), 7.56 (d, $J = 8.8$ Hz, 4H), 6.92 (d, $J = 8.8$ Hz, 4H), 6.50 (d, $J = 15.5$ Hz, 2H), 5.96 (s, 2H), 4.02 (t, $J = 6.4$ Hz, 4H), 2.32 (s, 6H), 1.87 – 1.75 (m, 4H), 1.53 – 1.36 (m, 8H). ^{13}C NMR (100 MHz, CDCl_3 , ppm): $\delta = 180.9$, 162.9, 148.8, 131.6, 129.0, 126.5, 117.0, 115.4, 101.2, 28.4, 29.3, 29.1, 26.0, 24.4.



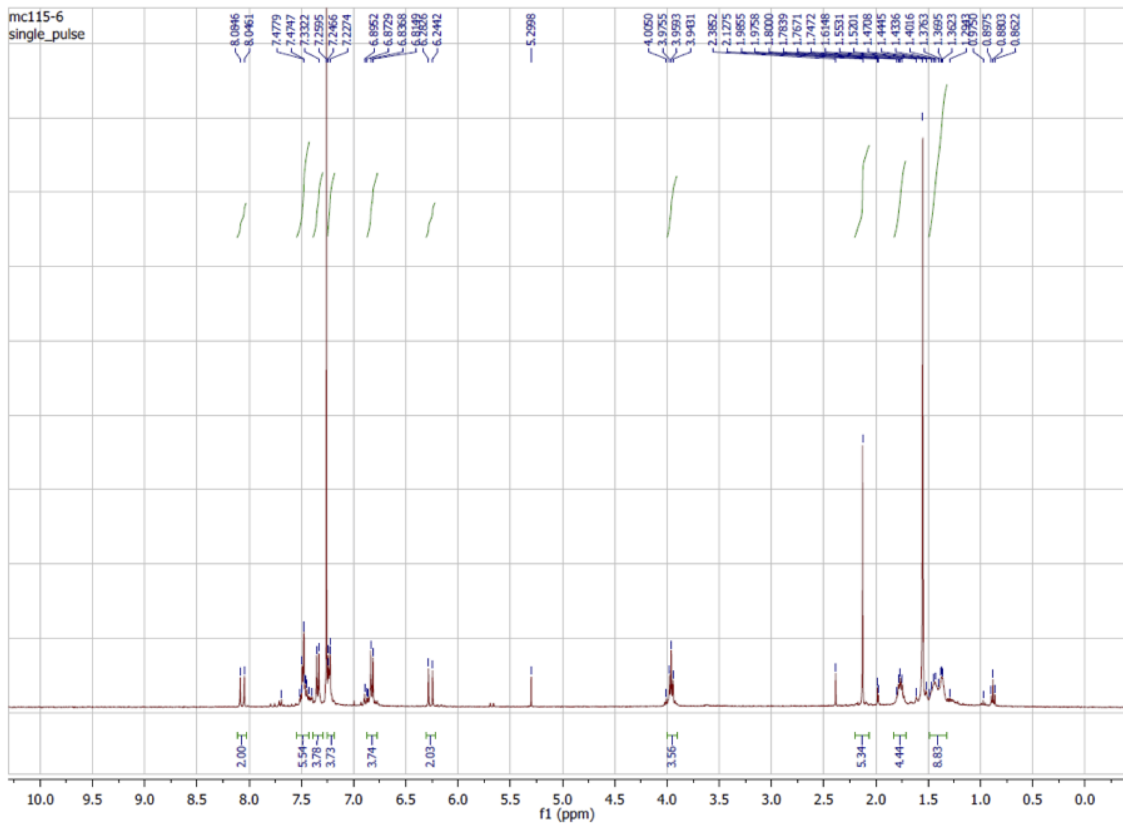


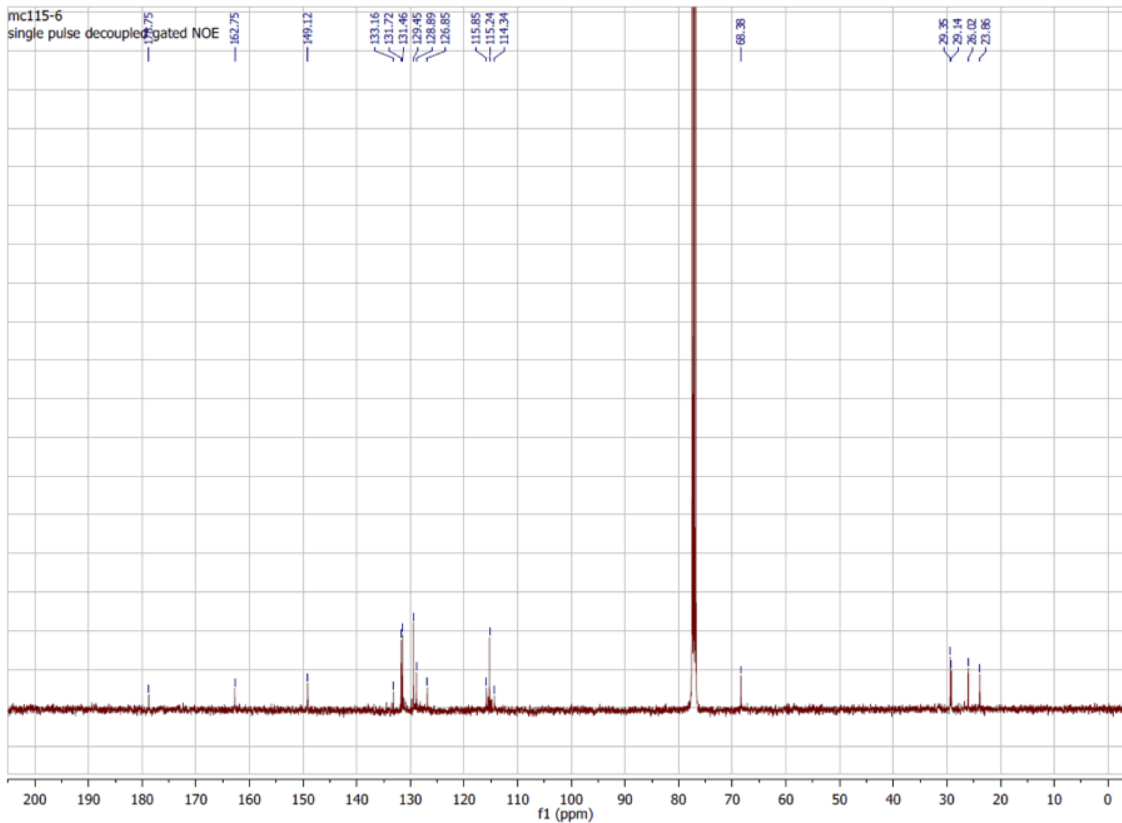
1.4 BF₂-hemicurcuminoid H3



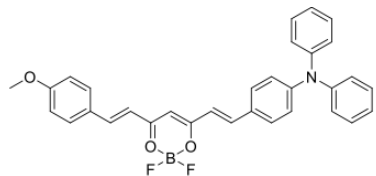
Difluoro(3-phenylpentane-2,4-dionato)boron (4.0 g, 17.86 mmol) was dissolved into 50 mL of toluene and stirred at reflux for 30 min under argon. Solution of 1,8-bis(4-formylphenoxy)octane (1.58 g, 4.47 mmol) and tri-*n*-butylborate (1.45 mL, 5.36 mmol) in 100 mL of toluene was added dropwise into the reaction mixture. After stirring for 30 min at reflux, a first portion of *n*-butylamine (221 μ L, 2.24 mmol) was added to the reaction mixture. A second portion of *n*-butylamine (221 μ L, 2.24 mmol) was added after 2h and the reaction mixture was stirred

at reflux overnight. After cooling, the precipitate was filtered under vacuum. The product was purified on silica gel column with cyclohexane/dichloromethane (7/3 v:v) as eluent to give the product as an orange powder (452 mg, 15 %). ^1H NMR (400 MHz, CDCl_3 , ppm): δ = 8.07 (d, J = 15.4 Hz, 2H), 7.54 – 7.42 (m, 6H), 7.34 (d, J = 8.8 Hz, 4H), 7.26 – 7.21 (m, 4H), 6.83 (d, J = 8.8 Hz, 4H), 6.26 (d, J = 15.4 Hz, 2H), 3.96 (t, J = 6.5 Hz, 4H), 2.13 (s, 6H), 1.82 – 1.71 (m, 4H), 1.51 – 1.31 (m, 8H). ^{13}C NMR (100 MHz, CDCl_3 , ppm): δ = 178.8, 162.8, 149.1, 133.2, 131.8, 131.5, 129.5, 128.9, 126.9, 115.9, 115.2, 114.3, 68.4, 29.4, 29.1, 26.0, 23.9.



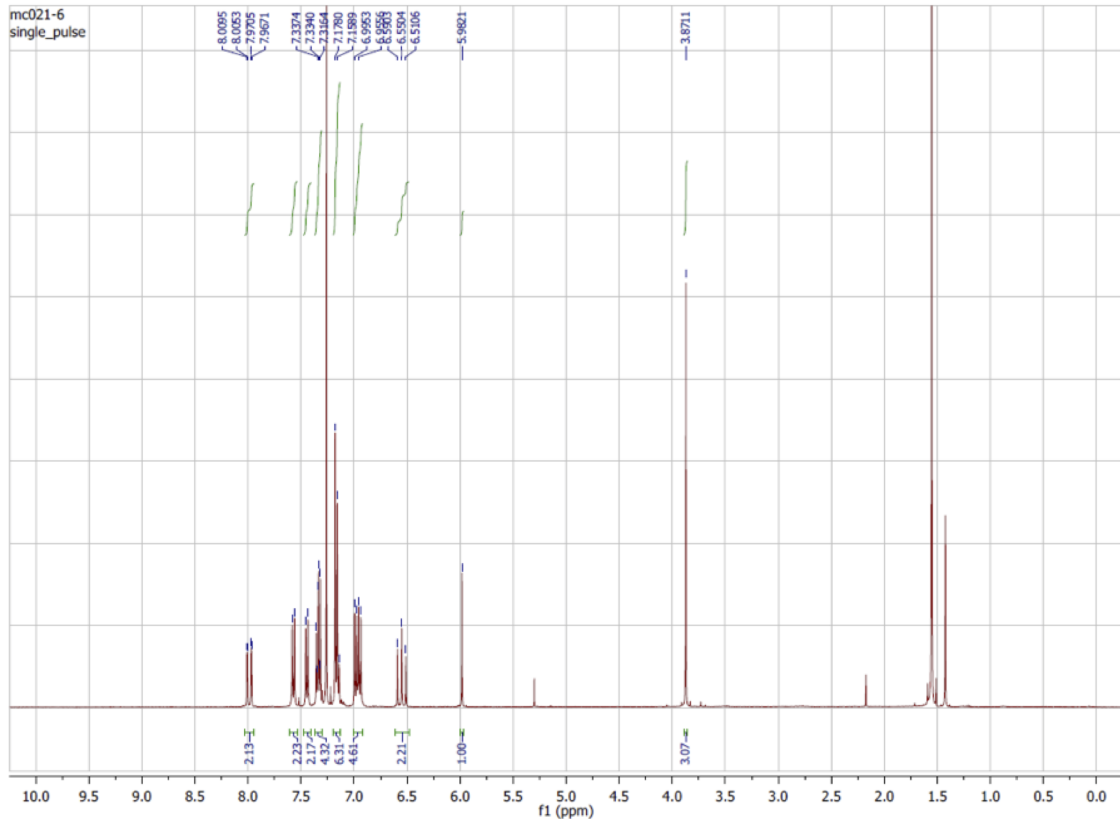


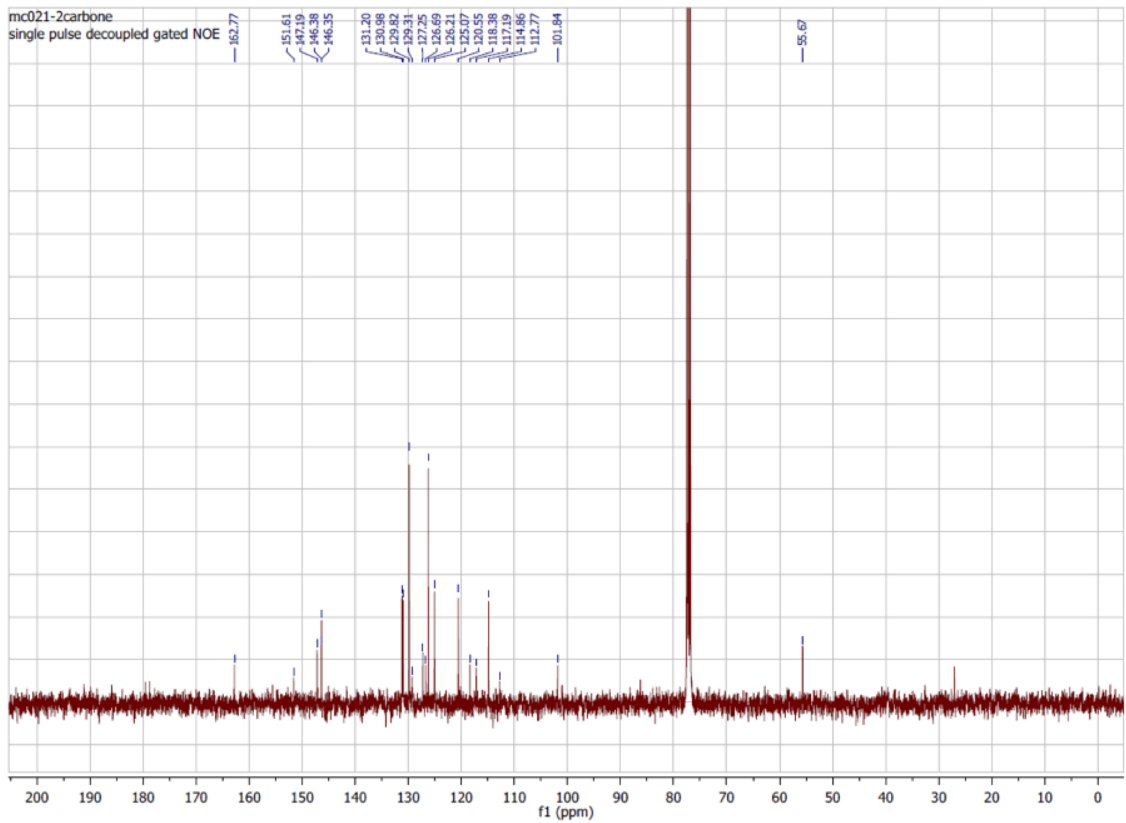
1.5 Monomer 2



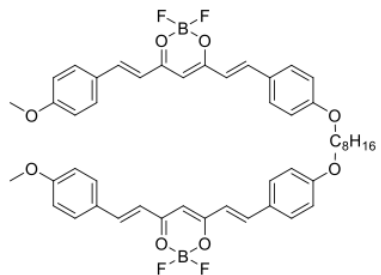
BF_3 -hemicurcuminoid **H1** (0.5 g, 1.88 mmol) was dissolved into 30 mL of ethyl acetate and heated to 60 °C. A solution of 4-(*N,N*-diphenylamino)benzaldehyde (0.62 g, 2.26 mmol) and tri-*n*-butylborate (612 μL , 2.26 mmol) in 30 mL of ethyl acetate was added to the reaction mixture and stirred for a further 30 min at 60 °C. Then, *n*-butylamine (74.3 μL , 0.75 mmol) was added to the solution. A second portion of the *n*-butylamine was made (37.2 μL , 0.38 mmol) after 4h. The reaction mixture was stirred at 60 °C overnight. After cooling, the solvent was removed under vacuum and the crude was purified on silica gel column with cyclohexane/dichloromethane (1/1 v:v) as eluent. Precipitation from cyclohexane/dichloromethane gave the product as a brown powder (122 mg, 12 %). ^1H NMR (400 MHz, CDCl_3 , ppm): δ = 7.99 (d, J = 15.6 Hz, 1H), 7.98 (d, J = 15.3 Hz, 1H), 7.57 (d,

$J = 8.8$ Hz, 2H), 7.44 (d, $J = 8.8$ Hz, 2H), 7.37 – 7.30 (m, 4H), 7.20 – 7.12 (m, 6H), 6.98 (d, $J = 8.8$ Hz, 2H), 6.94 (d, $J = 8.8$ Hz, 2H), 6.57 (d, $J = 15.6$ Hz, 1H), 6.53 (d, $J = 15.3$ Hz, 1H), 5.98 (s, 1H), 3.87 (s, 3H). ^{13}C NMR (100 MHz, CDCl_3 , ppm): $\delta = 179.5, 178.8, 162.8, 151.6, 147.2, 146.4, 146.3, 131.2, 131.0, 129.8, 127.3, 126.7, 126.2, 125.1, 120.6, 118.4, 117.2, 114.9, 101.9, 55.7$. HRMS (ESI): Calcd. For $\text{C}_{32}\text{H}_{26}\text{NO}_3\text{F}_2\text{BNa}^+ [\text{M}+\text{Na}]^+$: 544.1871. Found: 544.1872 (-0.2 ppm).



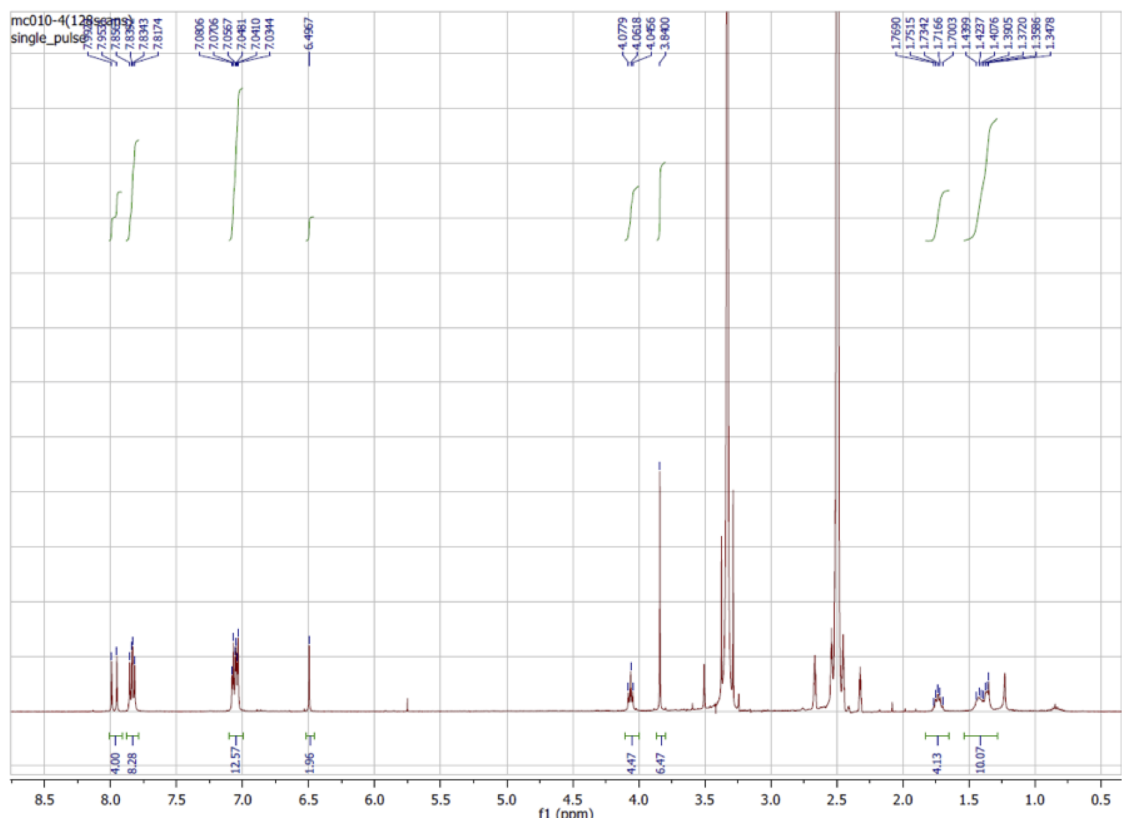


1.6 Dimer 1

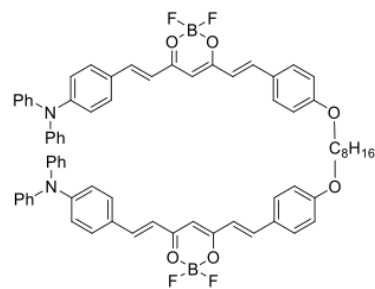


BF_3 -hemicurcuminoid **H1** (1.0 g, 3.76 mmol) was dissolved into 15 mL of ethyl acetate and heated to 60 °C. 1,8-Bis(4-formylphenoxy)octane (0.48 g, 1.50 mmol) and tri-*n*-butylborate (810 μL , 3.00 mmol) were dissolved into 10 mL of ethyl acetate and the solution was added to the reaction mixture. After 30 min at 60°C, a first portion of *n*-butylamine (75 μL , 0.75 mmol) was added to the solution. A second portion of *n*-butylamine (75 μL , 0.75 mmol) was made after 2 h. After cooling, the precipitate was filtered under vacuum. The product was purified on silica gel column with dichloromethane as eluent (0.37 g, 32 %). ^1H NMR (400 MHz, DMSO, ppm): $\delta = 7.97$ (d, $J = 15.6$, 4H), 7.85 (d, $J = 8.8$, 4H), 7.83 (d, $J = 8.8$,

4H), 7.10 – 7.01 (m, 12H), 6.50 (s, 2H), 4.06 (t, J = 6.4, 4H), 3.84 (s, 6H), 1.80 – 1.67 (m, 4H), 1.48 – 1.31 (m, 8H). HRMS (ESI): Calcd. For $C_{48}H_{48}O_8F_4B_2Na^+$ [M+Na]⁺: 873.3380. Found: 873.3379 (+ 0.1 ppm).

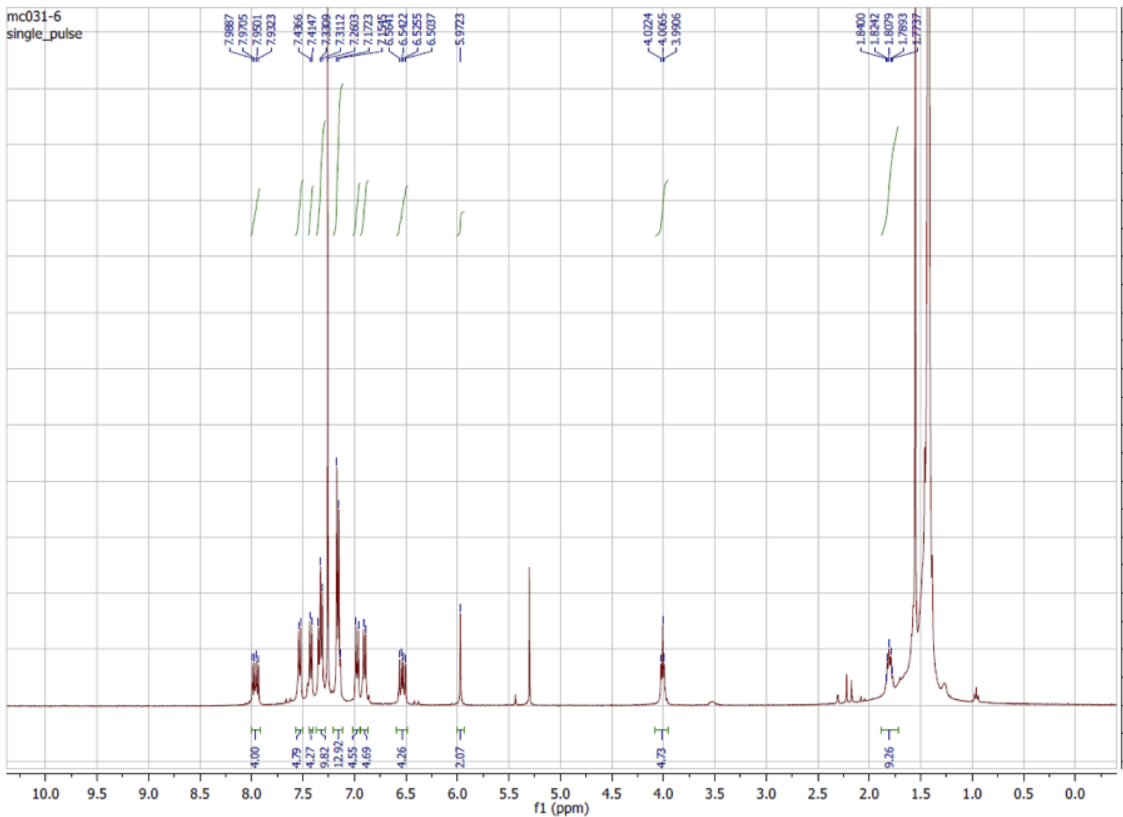


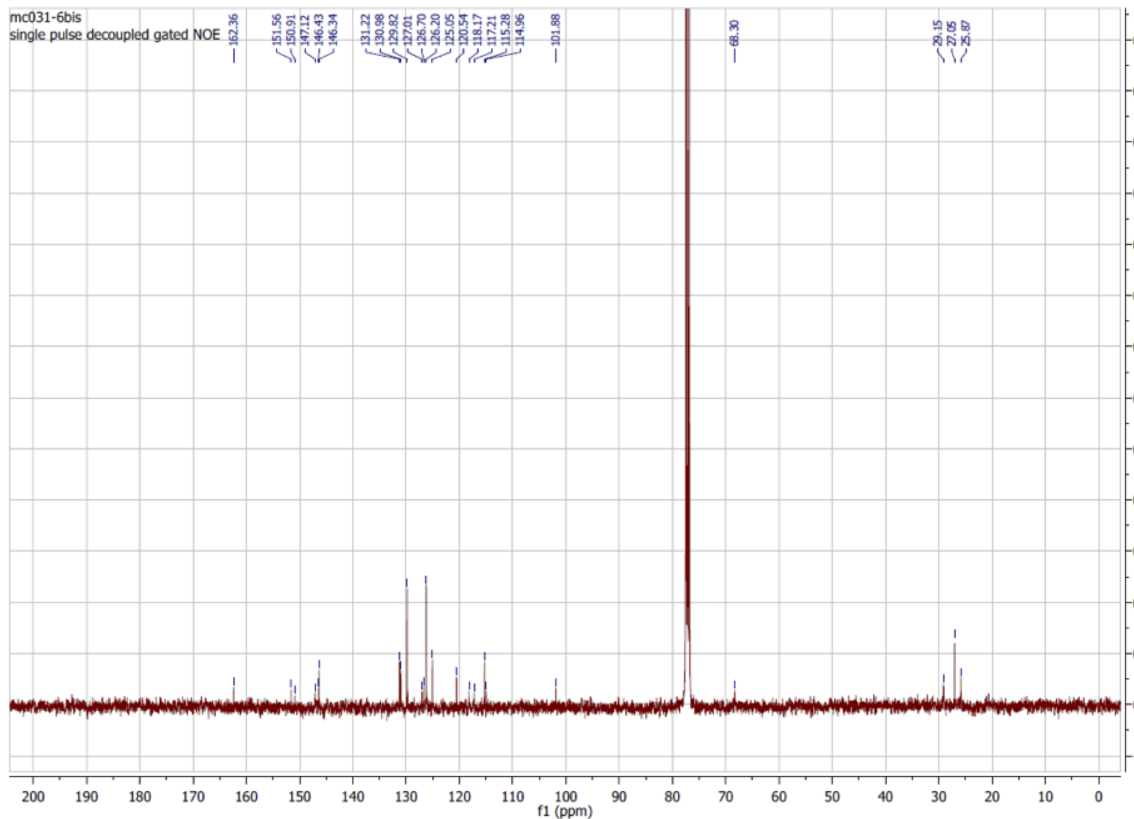
1.7 Dimer 2



BF₂-hemicurcuminoid H2 (0.78 g, 1.27 mmol) was dissolved into 20 mL of toluene and stirred at reflux. 4-(*N,N*-Diphenylamino)-benzaldehyde (0.70 g, 2.54 mmol) and tri-*n*-butylborate (687 μ L, 2.54 mmol) were dissolved into 40 mL of toluene and added to the reaction mixture. *n*-Butylamine (62.0 μ L, 0.63 mmol) was added after 30 min at reflux. A second addition

of the *n*-butylamine (62.0 μ L, 0.63 mmol) was made after 2 h. The reaction mixture was stirred at reflux overnight. After cooling, the solvent was removed under vacuum and the crude was purified on silica gel column with cyclohexane/dichloromethane (1/1 v:v) as eluent. The precipitation from cyclohexane/dichloromethane gave the product as a brown powder (144 mg, 11 %). ^1H NMR (400 MHz, CDCl_3 , ppm): δ = 7.97 (d, J = 15.4 Hz, 2H), 7.95 (d, J = 15.4 Hz, 2H), 7.53 (d, J = 8.7 Hz, 4H), 7.43 (d, J = 8.8 Hz, 4H), 7.37 – 7.29 (m, 8H), 7.20 – 7.12 (m, 12H), 6.97 (d, J = 8.7 Hz, 4H), 6.90 (d, J = 8.8 Hz, 4H), 6.54 (d, J = 15.4 Hz, 2H), 6.51 (d, J = 15.4 Hz, 2H), 5.97 (s, 2H), 4.01 (t, J = 6.4 Hz, 4H), 1.88 – 1.74 (m, 4H), 1.49 – 1.36 (m, 8H). ^{13}C NMR (100 MHz, CDCl_3 , ppm): δ = 162.4, 151.6, 150.9, 147.1, 146.4, 131.2, 131.0, 129.8, 127.0, 126.7, 126.2, 125.1, 120.5, 118.2, 117.2, 115.3, 115.0, 101.8, 68.3, 29.2, 27.1, 25.9. HRMS (ESI): Calcd. For $\text{C}_{70}\text{H}_{62}\text{N}_2\text{O}_6\text{F}_4\text{B}_2\text{Na}^+$ [M+Na] $^+$: 1147.4644. Found: 1147.4648 (+0.3 ppm).





1.8 Absorption spectra of monomers **1** and **2** in different solvents

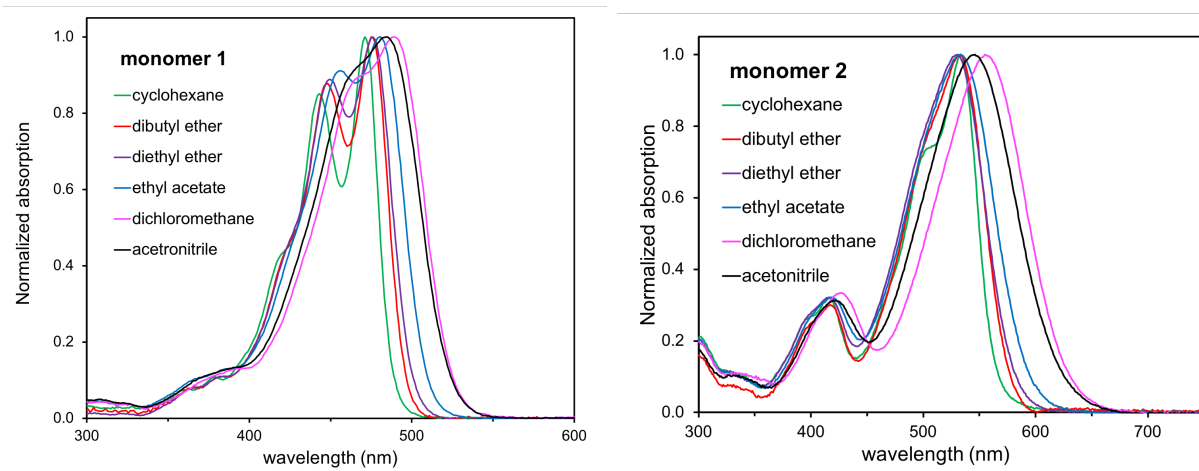


Figure S1: Normalized absorption spectra of curcumin monomers **1** (left) and **2** (right) recorded in different solvents.

2 Excitation energies: functional and basis set

2.1 Curcumin monomers

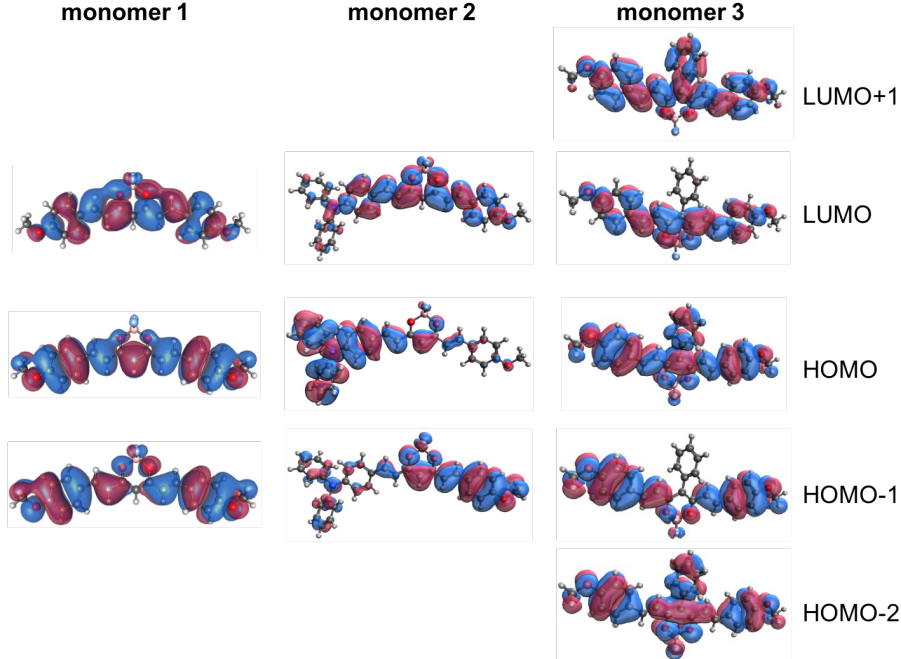


Figure S2: Frontier molecular orbitals of the curcumin monomers **1-3** calculated at the ω B97X-D/6-31+G(d) level. Molecular orbitals of **3** corresponds to the $\theta = 62^\circ$ case.

Table S1: Excitation energies (in eV) of monomer **1** obtained with different energy functionals and the 6-31+G(d) basis set in vacuum. Oscillator strengths indicated in parenthesis.

state	ω B97X-D		BLYP		B3LYP		CAM-B3LYP	
	TDA	TDDFT	TDA	TDDFT	TDA	TDDFT	TDA	TDDFT
S_1	3.43 (2.47)	3.32 (2.13)	2.58 (1.75)	2.47 (1.42)	2.98 (2.30)	2.86 (2.25)	3.37 (2.48)	3.26 (2.11)
S_2	4.34 (0.10)	4.15 (0.08)	2.74 (0.02)	2.68 (0.02)	3.42 (0.00)	3.33 (0.02)	4.24 (0.09)	4.05 (0.07)

Table S2: Excitation energies (in eV) of monomer **1** computed with the ω B97X-D functional and different basis sets. Oscillator strengths indicated in parenthesis.

state	6-31+G(d)		6-311++G(d,p)	
	TDA	TDDFT	TDA	TDDFT
S_1	3.43 (2.47)	3.32 (2.13)	3.42 (2.46)	3.30 (2.13)
S_2	4.34 (0.10)	4.15 (0.08)	4.32 (0.10)	4.13 (0.08)

Table S3: Excitation energies (in eV) of monomer **2** obtained with different energy functionals and the 6-31+G(d) basis set in vacuum. Oscillator strengths indicated in parenthesis.

	ω B97X-D		B3LYP		CAM-B3LYP	
	TDA	TDDFT	TDA	TDDFT	TDA	TDDFT
S_1	3.82 (1.33)	3.73 (1.32)	2.94 (0.98)	2.82 (0.98)	3.75 (1.28)	3.72 (1.28)
S_2	4.00 (0.99)	3.91 (1.00)	3.30 (0.75)	3.18 (0.78)	3.97 (0.98)	3.93 (0.97)

Table S4: Excitation energies (in eV) of monomer **3** obtained with different energy functionals and the 6-31+G(d) basis set in vacuum. Oscillator strengths indicated in parenthesis.

	ω B97X-D		B3LYP	
	TDA	TDDFT	TDA	TDDFT
S_1	3.07 (1.02)	3.00 (0.92)	2.56 (0.80)	2.43 (0.79)
S_2	4.04 (1.20)	3.96 (1.19)	3.18 (1.01)	3.14 (0.96)
S_3	4.14 (0.02)	4.08 (0.01)	3.21 (0.02)	3.16 (0.20)

Table S5: Main orbital contributions (in %) for the low-lying singlet excitations of monomers **1-3** computed at the TDA level with B3LYP and ω B97X-D energy functionals and the 6-31+G(d) basis set in vacuum. H and L indicate HOMO and LUMO, respectively.

comp.	state	ω B97X-D	B3LYP	transition
1	S_1	88	87	H→L
	S_2	83	85	H-1→L
2	S_1	63	68	H→L
		23	18	H-1→L
	S_2	70	20	H-1→L
		12	11	H→L
3	S_1	94	92	H→L
	S_2	78	83	H-2→L
	S_3	56	51	H-1→L
		39	37	H→L+1

2.2 Curcumin derivative dimers

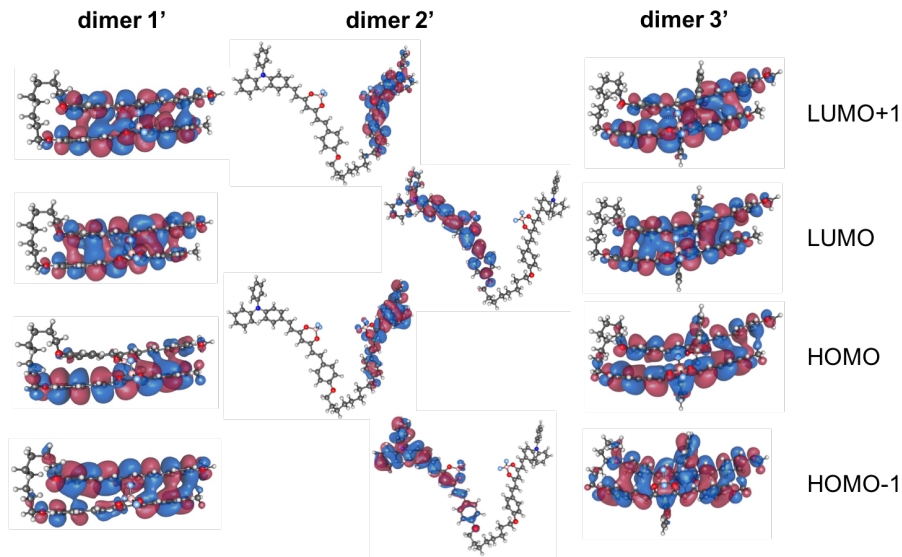


Figure S3: Frontier molecular orbitals of the curcumin dimers **1'**-**3'** calculated at the ω B97X-D/6-31+G(d) level.

Table S6: Excitation energies (in eV) of dimer **1'** (folded) obtained with different energy functionals and the 6-31+G(d) basis set in vacuum. Oscillator strengths indicated in parenthesis.

state	ω B97X-D		B3LYP	
	TDA	TDDFT	TDA	TDDFT
S_1	3.03 (0.02)	2.96 (0.02)	2.48 (0.01)	2.35 (0.02)
S_2	3.39 (2.56)	3.27 (3.22)	2.90 (2.34)	2.78 (2.30)
S_3	3.52 (1.27)	3.47 (0.56)	3.03 (1.08)	2.86 (1.18)
S_4	3.64 (1.27)	3.57 (0.37)	3.10 (1.08)	2.97 (1.18)
S_5	4.02 (0.09)	3.94 (0.06)	3.28 (0.06)	3.06 (0.01)
S_6	4.11 (0.01)	4.05 (0.01)	3.33 (0.01)	3.16 (0.04)
S_7	4.31 (0.02)	4.28 (0.02)	3.39 (0.00)	3.26 (0.00)
S_8	4.41 (0.01)	4.38 (0.01)	3.41 (0.00)	3.32 (0.00)

Table S7: Excitation energies (in eV) of dimer **2'** (V-shape) obtained with different energy functionals and the 6-31+G(d) basis set in vacuum. Oscillator strengths indicated in parenthesis.

state	ω B97X-D		B3LYP		CAM-B3LYP	
	TDA	TDDFT	TDA	TDDFT	TDA	TDDFT
S_1	3.81 (1.46)	3.80 (1.45)	2.92 (1.17)	2.91 (1.17)	3.73 (1.96)	3.71 (1.95)
S_2	3.81 (1.46)	3.80 (1.45)	2.95 (1.22)	2.95 (1.21)	3.73 (1.91)	3.71 (1.94)
S_3	4.00 (0.96)	3.99 (0.96)	2.98 (0.40)	2.96 (0.41)	4.00 (0.90)	3.99 (0.89)
S_4	4.00 (0.96)	3.99 (0.96)	3.04 (0.41)	3.04 (0.41)	4.00 (0.87)	3.99 (0.87)
S_5	4.32 (0.01)	4.33 (0.01)	3.22 (0.02)	3.22 (0.02)	4.34 (0.01)	4.32 (0.01)
S_6	4.34 (0.01)	4.34 (0.01)	3.24 (0.03)	3.24 (0.03)	4.35 (0.01)	4.32 (0.01)
S_7	4.45 (0.02)	4.42 (0.01)	3.25 (0.02)	3.25 (0.02)	4.45 (0.02)	4.42 (0.02)
S_8	4.45 (0.03)	4.43 (0.02)	3.28 (0.00)	3.28 (0.00)	4.46 (0.07)	4.43 (0.04)

Table S8: Excitation energies (in eV) of dimer **3'** (folded) obtained with different energy functionals and the 6-31+G(d) basis set in vacuum. Oscillators strengths indicated in parenthesis.

state	ω B97X-D		B3LYP	
	TDA	TDDFT	TDA	TDDFT
S_1	2.78 (0.02)	2.76 (0.01)	2.39 (0.01)	2.37 (0.01)
S_2	3.28 (2.51)	3.26 (2.50)	2.40 (2.32)	2.39 (2.32)
S_3	3.43 (1.58)	3.40 (1.58)	2.58 (1.49)	2.55 (1.59)
S_4	3.71 (0.11)	3.68 (0.09)	2.69 (0.08)	2.69 (0.06)
S_5	3.88 (0.28)	3.79 (0.19)	2.73 (0.12)	2.70 (0.09)
S_6	4.12 (0.07)	4.10 (0.05)	2.75 (0.03)	2.73 (0.02)
S_7	4.16 (0.07)	4.14 (0.06)	2.77 (0.03)	2.76 (0.03)
S_8	4.26 (0.02)	4.24 (0.02)	2.89 (0.02)	2.88 (0.01)
S_9	4.27 (0.01)	4.25 (0.01)	2.91 (0.01)	2.90 (0.01)
S_{10}	4.28 (0.00)	4.25 (0.00)	2.93 (0.00)	2.92 (0.01)

Table S9: Excitation energy (in eV) and oscillator strengths (in parenthesis) at B3LYP/6-31+G(d) level of theory in the gas phase and in DCM solution for the three different curcumin covalent dimers.

dimer	state	gas phase		DCM	
		TDDFT	TDA	TDDFT	TDA
1' (folded)	<i>S</i> ₁	2.35 (0.016)	2.48 (0.009)	2.19 (0.008)	2.28 (0.009)
	<i>S</i> ₂	2.78 (2.301)	2.90 (2.342)	2.59 (2.307)	2.63 (2.307)
	<i>S</i> ₃	2.86 (1.178)	3.03 (1.083)	2.68 (1.196)	2.74 (1.076)
	<i>S</i> ₄	2.97 (1.182)	3.10 (1.085)	2.71 (1.192)	3.80 (1.091)
	<i>S</i> ₅	3.06 (0.010)	3.28 (0.059)	2.87 (0.022)	2.96 (0.032)
	<i>S</i> ₆	3.16 (0.045)	3.33 (0.005)	2.98 (0.007)	3.04 (0.004)
	<i>S</i> ₇	3.26 (0.002)	3.39 (0.001)	3.03 (0.001)	3.13 (0.001)
	<i>S</i> ₈	3.32 (0.001)	3.41 (0.000)	3.11 (0.000)	3.20 (0.000)
2' (V-shape)	<i>S</i> ₁	2.91 (1.172)	2.92 (1.169)	2.40 (1.171)	2.41 (1.170)
	<i>S</i> ₂	2.95 (1.211)	2.95 (1.221)	2.49 (1.222)	2.49 (1.220)
	<i>S</i> ₃	2.96 (0.401)	2.98 (0.401)	2.58 (0.402)	2.60 (0.400)
	<i>S</i> ₄	3.04 (0.406)	3.04 (0.389)	2.59 (0.401)	2.63 (0.399)
	<i>S</i> ₅	3.22 (0.017)	3.22 (0.009)	2.67 (0.013)	2.67 (0.009)
	<i>S</i> ₆	3.24 (0.028)	3.27 (0.028)	2.70 (0.026)	2.73 (0.021)
	<i>S</i> ₇	3.25 (0.021)	3.28 (0.010)	2.80 (0.023)	2.82 (0.019)
	<i>S</i> ₈	3.28 (0.002)	3.28 (0.012)	2.82 (0.002)	2.84 (0.002)
3' (folded)	<i>S</i> ₁	2.37 (0.009)	2.39 (0.010)	2.20 (0.009)	2.29 (0.011)
	<i>S</i> ₂	2.39 (2.319)	2.40 (2.320)	2.23 (2.302)	2.30 (2.324)
	<i>S</i> ₃	2.55 (1.487)	2.58 (1.488)	2.40 (1.489)	2.49 (1.490)
	<i>S</i> ₄	2.69 (0.063)	2.69 (0.076)	2.55 (0.071)	2.63 (0.074)
	<i>S</i> ₅	2.70 (0.086)	2.73 (0.120)	2.56 (0.089)	2.64 (0.096)
	<i>S</i> ₆	2.73 (0.021)	2.75 (0.026)	2.60 (0.021)	2.69 (0.022)
	<i>S</i> ₇	2.76 (0.028)	2.77 (0.027)	2.61 (0.026)	2.71 (0.029)
	<i>S</i> ₈	2.88 (0.014)	2.89 (0.019)	2.71 (0.021)	2.79 (0.017)
	<i>S</i> ₉	2.90 (0.012)	2.91 (0.009)	2.75 (0.011)	2.81 (0.010)
	<i>S</i> ₁₀	2.92 (0.006)	2.93 (0.003)	2.78 (0.001)	2.82 (0.001)

Table S10: Main orbital contributions (in %) for the low-lying singlet excitations of dimers **1'-3'** computed at the TDA level with B3LYP and ω B97X-D energy functionals and the 6-31+G(d) basis set in vacuum. H and L indicate HOMO and LUMO, respectively.

comp.	state	ω B97X-D	B3LYP	transition
1'	S_1	78	75	H-1→L
		18	19	H→L
	S_2	56	55	H→L
		26	27	H-1→L
	S_3	58	62	H→L+1
		20	30	H→L
	S_4	83	78	H-1→L+1
2'	S_1	76	80	H-1→L
	S_2	82	85	H→L+1
3'	S_1	41	43	H→L
		7	6	H-1→L
	S_2	49	47	H→L
		32	36	H-1→L
	S_3	47	45	H→L+1
		28	31	H→L
	S_4	34	31	H→L+1
		13	15	H-1→L

3 Rotation of the *meso*-phenyl in monomer 3

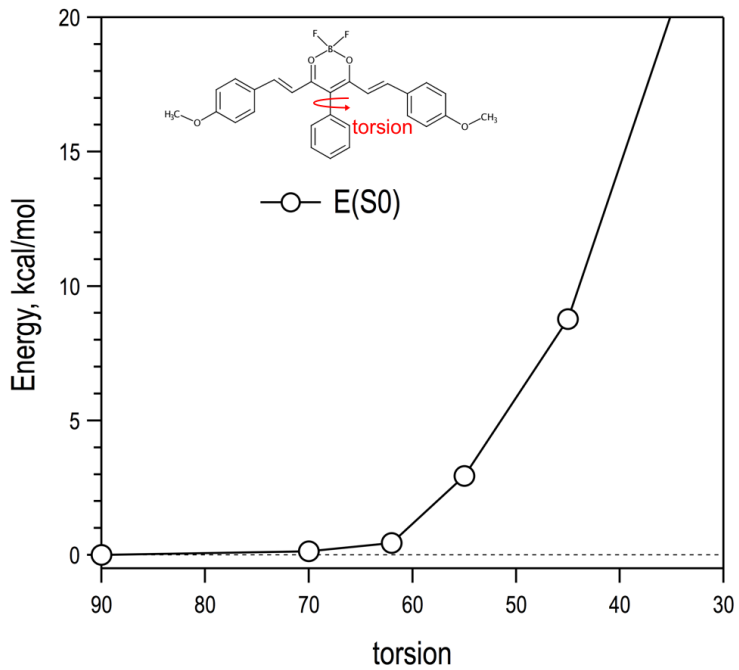


Figure S4: Ground state potential energy profile along the torsion of the *m*Ph group of monomer **3** computed at the B3LYP/6-31+G(d) level in DCM solution.

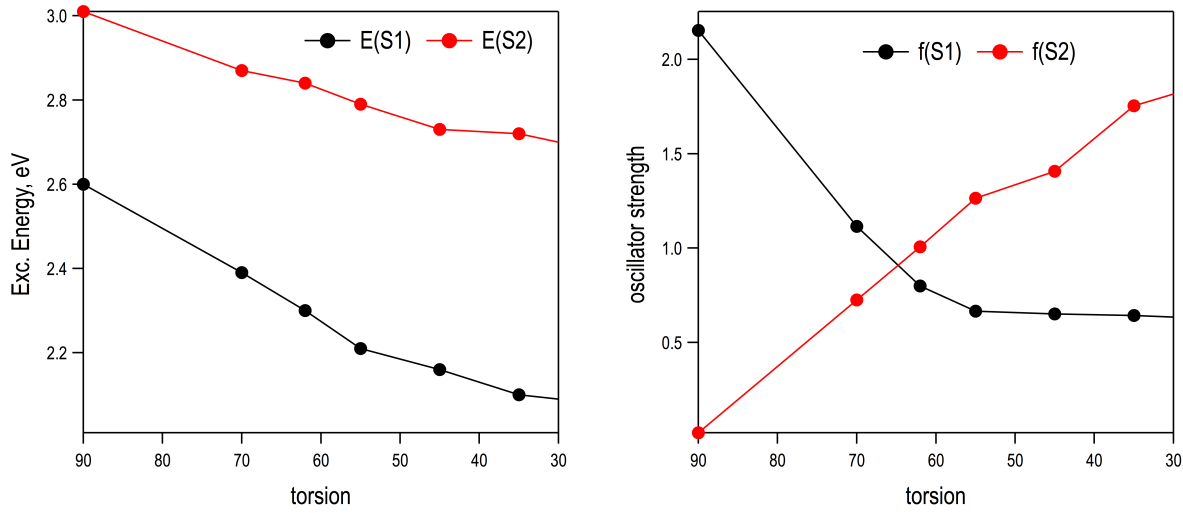


Figure S5: Excitation energies (left) and oscillator strengths (right) for the two lowest excited singlet states of **3** along the torsion of the *m*Ph group computed at the B3LYP/6-31+G(d) level in DCM solution.

4 Relative energies between open/folded conformers

The relative stability between opened and folded structural conformations of curcumin derivative covalent dimers is dictated by the competition between the solvent-chromophore interactions and the π -stacking between the two monomers. As a result, apolar solvents like cyclohexane show a higher preference towards the folded form compared with more polar solvents.

The relative energy between the two forms ($\Delta E = E(\text{open}) - E(\text{folded})$) has been computed in different solvents. Basis set superposition error (BSSE) have been corrected through the counterpoise procedure. To perform CP in covalent dimers we evaluate the CP correction at the folded from without the linker as:

$$E_{cp} = 2(E^*(\text{mono})) - E(\text{mono}) \quad (\text{S.1})$$

where $E(\text{mono})$ is the energy of the monomer, and $E^*(\text{mono})$ is the energy of the monomer in the presence of basis set functions in the positions of the second monomer in the folded form. Then, the corrected energy for the open conformer is obtained as:

$$E^c(\text{open}) = E(\text{open}) + E_{cp} \quad (\text{S.2})$$

Relative energies in different solvent are shown in Figure S6.

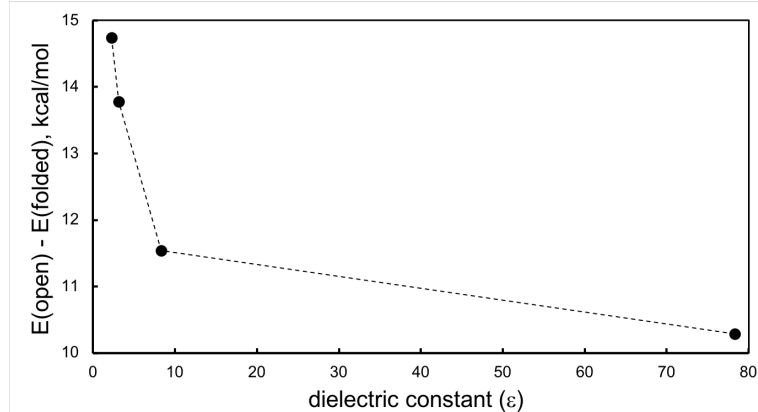


Figure S6: Computed relative stability (in kcal/mol) between the open and folded conformers of dimer **1'** as a function of the polarity of the solvent. Points at the graph correspond to the dielectric constants of benzene, Bu_2O , DCM and water (in increasing order of ϵ).

Our results systematically indicate a preference for the folded conformation of dimer **1'**. These results should not be taken quantitatively, since entropic effects (stabilizing the open form) are not included. On the other hand, the trend of relative energies demonstrates how

increasing the solvent's polarity shifts the equilibrium between the two forms towards the open conformation.

5 Absorption spectra: vibronic resolution

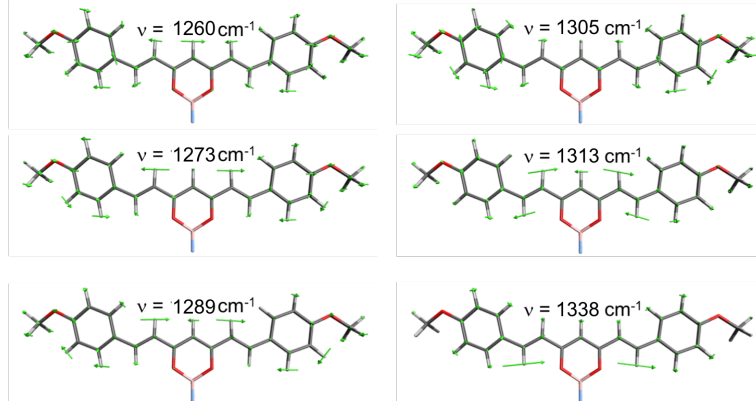


Figure S7: Frequency modes of **1** computed at the ω B97X-D potentially involved in the vibronic profile of absorption spectra (experimental vibronic gap $\sim 1260 \text{ cm}^{-1}$).

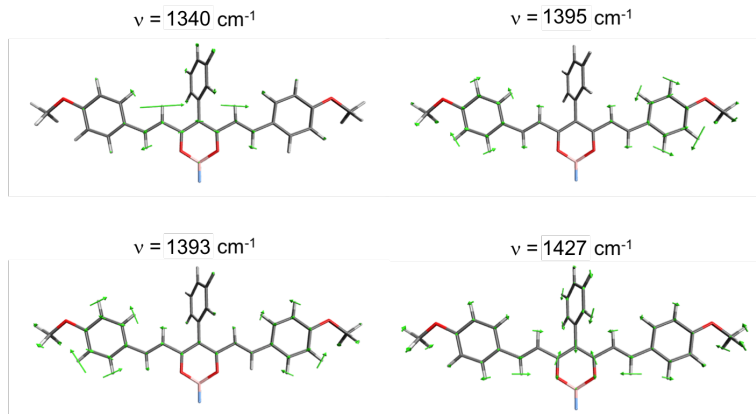


Figure S8: Frequency modes of **3** computed at the ω B97X-D potentially involved in the vibronic profile of absorption spectra (experimental vibronic gap $\sim 1320 \text{ cm}^{-1}$).

6 Diabatization of low-lying states

6.1 Diabatization scheme: Edmiston-Ruedenberg localization

Diabatic electronic states $\{|\Xi_i\rangle\}$ are obtained through the mixing of N adiabatic states $\{|\phi_j\rangle\}$ via a rotation matrix \mathbf{U} as:

$$|\Xi_i\rangle = \sum_{j=1}^N |\phi_j\rangle U_{ji}; \quad i = 1\dots N \quad (\text{S.3})$$

There are several techniques for generating the rotation matrix \mathbf{U} using a variety of different approaches. This rotation matrix is chosen by optimizing some diabatization function $f(\mathbf{U})$. In this case we use the Edmiston-Ruedenberg (ER) diabatization scheme, corresponding to the maximization of self-interaction energy:

$$f_{ER}(\mathbf{U}) = f_{ER}(\{|\Xi_i\rangle\}) = \sum_{j=1}^N \int d\mathbf{R}_1 \int d\mathbf{R}_2 \frac{\langle \Xi_i | \rho(\mathbf{R}_2) | \Xi_i \rangle \langle \Xi_i | \rho(\mathbf{R}_1) | \Xi_i \rangle}{|\mathbf{R}_1 - \mathbf{R}_2|} \quad (\text{S.4})$$

where the density operator at position \mathbf{R} is

$$\rho(\mathbf{R}) = \sum_j \delta(\mathbf{R} - \mathbf{r}^{(j)}) \quad (\text{S.5})$$

and $\mathbf{r}^{(j)}$ represents the position of the j -th electron.

6.2 Decomposition in the diabatic basis: dimers

Table S11: Contributions (in %) of the diabatic states (Z_{inter} and Z_{intra}) for the eight lowest adiabatic states (S_i , $i = 1, 8$) of dimer **1'**.

state	Z_{inter}	Z_{intra}
S_1	67	33
S_2	74	26
S_3	66	34
S_4	23	77
S_5	54	46
S_6	33	67
S_7	34	66
S_8	49	51

Table S12: Contributions (in %) of the diabatic states for the ten lowest adiabatic states (S_i , $i = 1, 10$) of dimer **3'**. $Z_{\text{inter}} = Z_2 + Z_3 + Z_7 + Z_8$, $Z_{\text{intra}} = Z_1 + Z_4 + Z_9 + Z_{10}$ and $Z_{\text{meso}} = Z_5 + Z_6$.

state	Z_{inter}	Z_{intra}	Z_{meso}
S_1	60	38	2
S_2	72	27	1
S_3	14	86	0
S_4	11	89	0
S_5	22	20	58
S_6	46	18	36
S_7	43	32	25
S_8	31	7	62
S_9	22	70	8
S_{10}	80	10	10

6.3 Electronic Hamiltonians

By definition, the adiabatic states of a system $\{|\phi_j\rangle\}$ are those electronic states that diagonalize the electronic Hamiltonian, assuming that the nuclei are fixed. The spectrum ($\{E_j\}$) of these adiabatic states yields fixed-nuclei energies for the ground and excited electronic states of a system. The off-diagonal elements of the Hamiltonian ($H_{ij} = \langle Z_i | \hat{H} | Z_j \rangle$) are known as *electronic couplings*.

6.3.1 Electronic Hamiltonians of curcumin monomers

Diabatic Hamiltonian (\mathbf{H}_{diab}) and adiabatic energies (\mathbf{E}_{ad}) for curcumin derivative **1** computed at the B3LYP/6-31+G(d) level within TDA in vacuum (values in eV):

$$\mathbf{H}_{\text{diab}} = \begin{bmatrix} 3.22 & 0.22 \\ 0.22 & 3.22 \end{bmatrix}; \quad \mathbf{E}_{\text{ad}} = \begin{bmatrix} 2.98 \\ 3.42 \end{bmatrix} \quad (\text{S.6})$$

Diabatic Hamiltonian (\mathbf{H}_{diab}) and adiabatic energies (\mathbf{E}_{ad}) for curcumin derivative **2** computed at the B3LYP/6-31+G(d) level within TDA in vacuum (values in eV):

$$\mathbf{H}_{\text{diab}} = \begin{bmatrix} 2.94 & 0.02 \\ 0.02 & 3.30 \end{bmatrix}; \quad \mathbf{E}_{\text{ad}} = \begin{bmatrix} 2.94 \\ 3.30 \end{bmatrix} \quad (\text{S.7})$$

Diabatic Hamiltonian (\mathbf{H}_{diab}) and adiabatic energies (\mathbf{E}_{ad}) for curcumin derivative **3** ($\theta = 90^\circ$) computed at the B3LYP/6-31+G(d) level within TDA in vacuum (values in eV):

$$\mathbf{H}_{\text{diab}} = \begin{bmatrix} 3.25 & 0.33 & -0.02 \\ 0.33 & 3.25 & 0.02 \\ -0.02 & 0.02 & 3.32 \end{bmatrix}; \quad \mathbf{E}_{\text{ad}} = \begin{bmatrix} 2.92 \\ 3.32 \\ 3.59 \end{bmatrix} \quad (\text{S.8})$$

Diabatic Hamiltonian (\mathbf{H}_{diab}) and adiabatic energies (\mathbf{E}_{ad}) for curcumin derivative **3** ($\theta = 62^\circ$) computed at the B3LYP/6-31+G(d) level within TDA in vacuum (values in eV):

$$\mathbf{H}_{diab} = \begin{bmatrix} 3.11 & 0.33 & 0.04 \\ 0.33 & 3.11 & -0.04 \\ 0.04 & -0.04 & 2.72 \end{bmatrix}; \mathbf{E}_{ad} = \begin{bmatrix} 2.56 \\ 3.18 \\ 3.21 \end{bmatrix} \quad (\text{S.9})$$

6.3.2 Electronic Hamiltonians of curcumin dimers

Diabatic Hamiltonian (\mathbf{H}_{diab}) and adiabatic energies (\mathbf{E}_{ad}) for curcumin derivative dimer **1'** computed at the B3LYP/6-31+G(d) level within TDA in vacuum (values in eV):

$$\mathbf{H}_{diab} = \begin{bmatrix} 3.15 & 0.20 & 0.02 & 0.00 & 0.03 & 0.13 & -0.18 & -0.07 \\ 0.20 & 3.15 & 0.00 & 0.11 & 0.01 & 0.03 & 0.04 & 0.15 \\ 0.02 & 0.00 & 3.15 & 0.20 & 0.11 & 0.14 & -0.15 & -0.03 \\ 0.00 & 0.11 & 0.20 & 3.15 & 0.11 & -0.08 & -0.03 & -0.02 \\ 0.03 & 0.01 & 0.11 & 0.11 & 3.20 & 0.11 & 0.14 & -0.05 \\ 0.13 & 0.03 & 0.14 & -0.08 & 0.11 & 3.20 & 0.11 & -0.16 \\ -0.18 & 0.04 & -0.15 & -0.03 & 0.14 & 0.11 & 3.29 & 0.09 \\ -0.07 & 0.15 & -0.03 & -0.02 & -0.05 & -0.16 & 0.09 & 3.29 \end{bmatrix}; \mathbf{E}_{ad} = \begin{bmatrix} 2.48 \\ 2.90 \\ 3.03 \\ 3.10 \\ 3.28 \\ 3.33 \\ 3.39 \\ 3.41 \end{bmatrix} \quad (\text{S.10})$$

Diabatic Hamiltonian (\mathbf{H}_{diab}) and adiabatic energies (\mathbf{E}_{ad}) for curcumin derivative dimer **2'** computed at the B3LYP/6-31+G(d) level within TDA in vacuum (values in eV):

$$\mathbf{H}_{diab} = \begin{bmatrix} 2.92 & 0.00 & 0.00 & 0.00 & 0.00 & 0.00 & 0.00 & 0.00 \\ 0.00 & 2.95 & 0.00 & 0.00 & 0.00 & 0.00 & 0.00 & 0.00 \\ 0.00 & 0.00 & 2.98 & 0.01 & 0.00 & 0.00 & 0.00 & 0.00 \\ 0.00 & 0.00 & 0.01 & 3.04 & 0.00 & 0.00 & 0.00 & 0.00 \\ 0.00 & 0.00 & 0.00 & 0.00 & 3.22 & 0.01 & 0.00 & 0.00 \\ 0.00 & 0.00 & 0.00 & 0.00 & 0.01 & 3.27 & 0.00 & 0.00 \\ 0.00 & 0.00 & 0.00 & 0.00 & 0.00 & 0.00 & 3.28 & 0.02 \\ 0.00 & 0.00 & 0.00 & 0.00 & 0.00 & 0.00 & 0.02 & 3.28 \end{bmatrix}; \mathbf{E}_{ad} = \begin{bmatrix} 2.92 \\ 2.95 \\ 2.98 \\ 3.04 \\ 3.22 \\ 3.27 \\ 3.28 \\ 3.28 \end{bmatrix} \quad (\text{S.11})$$

Diabatic Hamiltonian (\mathbf{H}_{diab}) and adiabatic energies (\mathbf{E}_{ad}) for curcumin derivative dimer **3'** computed at the B3LYP/6-31+G(d) level within TDA in vacuum (values in eV):

$$\mathbf{H}_{diab} = \begin{bmatrix} 2.50 & 0.00 & 0.00 & 0.12 & 0.00 & 0.00 & 0.00 & 0.00 & 0.00 & 0.00 & 0.00 \\ 0.00 & 2.60 & -0.19 & 0.00 & 0.00 & 0.00 & 0.00 & 0.00 & 0.00 & 0.00 & 0.00 \\ 0.00 & -0.19 & 2.62 & 0.00 & 0.00 & 0.00 & 0.00 & 0.00 & 0.00 & 0.00 & 0.00 \\ 0.12 & 0.00 & 0.00 & 2.66 & 0.00 & 0.00 & 0.00 & 0.00 & 0.00 & 0.00 & 0.00 \\ 0.00 & 0.00 & 0.00 & 0.00 & 2.72 & 0.16 & 0.00 & 0.00 & 0.00 & 0.00 & 0.00 \\ 0.00 & 0.00 & 0.00 & 0.00 & 0.16 & 2.73 & 0.00 & 0.00 & 0.00 & 0.00 & 0.00 \\ 0.00 & 0.00 & 0.00 & 0.00 & 0.00 & 0.00 & 2.77 & -0.09 & 0.07 & 0.07 & 0.07 \\ 0.00 & 0.00 & 0.00 & 0.00 & 0.00 & 0.00 & -0.09 & 2.77 & 0.07 & 0.07 & 0.07 \\ 0.00 & 0.00 & 0.00 & 0.00 & 0.00 & 0.00 & 0.07 & 0.07 & 2.78 & -0.08 & 0.07 \\ 0.00 & 0.00 & 0.00 & 0.00 & 0.00 & 0.00 & 0.07 & -0.08 & 0.07 & 2.79 & 0.07 \end{bmatrix}; \mathbf{E}_{ad} = \begin{bmatrix} 2.39 \\ 2.40 \\ 2.58 \\ 2.69 \\ 2.73 \\ 2.75 \\ 2.77 \\ 2.89 \\ 2.91 \\ 2.93 \end{bmatrix} \quad (S.12)$$

7 Fragment charge distribution

7.1 Curcumin derivatives: monomers

Table S13: Relative Mulliken fragment charges of **diabatic** states of curcumin monomers **1-3** with respect to the ground state charge distribution computed at the B3LYP/6-31+G(d) level.

Comp.	State	Fragment			
		PMP ₁	DOB	PMP ₂	
1	<i>Z</i> ₁	0.347	-0.322	-0.025	
	<i>Z</i> ₂	-0.031	-0.326	0.357	
2		TPA	DOB	PMP	
	<i>Z</i> ₁	0.450	-0.392	-0.057	
3	<i>Z</i> ₂	0.038	-0.374	0.343	
		PMP ₁	DOB	PMP ₂	<i>mPh</i>
3	<i>Z</i> ₁	0.345	-0.325	-0.020	0.000
	<i>Z</i> ₂	-0.020	-0.325	0.345	0.000
	<i>Z</i> ₃	0.042	-0.400	0.042	0.315
3	<i>Z</i> ₁	0.346	-0.323	-0.020	-0.002
	<i>Z</i> ₂	-0.001	-0.324	0.347	-0.010
	<i>Z</i> ₃	0.040	-0.394	0.050	0.302

Table S14: Relative Mulliken fragment charges of **adiabatic** states of curcumin monomers **1-3** with respect to the ground state charge distribution computed at the B3LYP/6-31+G(d) level.

Comp.	State	Fragment			
		PMP ₁	DOB	PMP ₂	
1	<i>S</i> ₁	0.113	-0.234	0.120	-
	<i>S</i> ₂	0.203	-0.415	0.212	-
2		TPA	DOB	PMP	
	<i>S</i> ₁	0.449	-0.391	-0.057	-
3	<i>S</i> ₁	0.021	-0.362	0.341	-
		PMP ₁	DOB	PMP ₂	<i>mPh</i>
3 $\theta = 90^\circ$	<i>S</i> ₁	0.110	-0.235	0.120	0.005
	<i>S</i> ₂	0.042	-0.400	0.042	0.315
	<i>S</i> ₃	0.205	-0.420	0.210	0.005
3 $\theta = 62^\circ$	<i>S</i> ₁	0.067	-0.330	0.066	0.190
	<i>S</i> ₂	0.142	-0.354	0.139	0.071
	<i>S</i> ₃	0.157	-0.346	0.156	0.033

7.2 Curcumin derivatives: dimers

Table S15: Relative Mulliken fragment charges of **diabatic** states of curcumin dimer **1'** (folded) with respect to the ground state charge distribution computed at the B3LYP/6-31+G(d) level. Nomenclature: PMP_{1a}-DOB₁-PMP_{1b}-(CH₂)₈-PMP_{2b}-DOB₂-PMP_{2a}.

diabat	Fragment					
	PMP _{1a}	DOB ₁	PMP _{1b}	PMP _{2a}	DOB ₂	PMP _{2b}
<i>Z</i> ₁	0.000	-0.310	0.012	0.000	-0.037	0.335
<i>Z</i> ₂	0.010	-0.310	0.000	0.340	-0.040	0.000
<i>Z</i> ₃	0.000	-0.036	0.338	0.000	-0.310	0.008
<i>Z</i> ₄	0.338	-0.026	0.000	0.001	-0.315	0.000
<i>Z</i> ₅	0.000	-0.111	0.111	0.109	-0.109	0.000
<i>Z</i> ₆	0.109	-0.110	0.000	0.000	-0.109	0.110
<i>Z</i> ₇	0.000	-0.110	0.110	0.000	-0.111	0.111
<i>Z</i> ₈	0.109	-0.109	0.000	0.110	-0.110	0.000

Table S16: Relative Mulliken fragment charges of **diabatic** states of curcumin dimer **2'** (V-shape) with respect to the ground state charge distribution computed at the B3LYP/6-31+G(d) level. Nomenclature: TPA₁-DOB₁-PMP₁-(CH₂)₈-PMP₂-DOB₂-TPA₂.

diabat	Fragments					
	TPA ₁	DOB ₁	PMP ₁	TPA ₂	DOB ₂	PMP ₂
Z _{1,Z₂}	0.450	-0.400	-0.050	0.450	-0.450	-0.050
Z _{3,Z₄}	0.210	-0.260	0.085	-0.018	-0.155	-0.100
Z _{5,Z₆}	0.145	-0.190	0.0520	-0.005	-0.210	0.100
Z _{7,Z₈}	0.030	-0.370	0.335	0.030	-0.370	0.335

Table S17: Mulliken analysis of the difference in charge in comparison to the ground state for the **adiabatic** states for the dimer **2'** (V-shape) computed at the B3LYP/6-31+G(d) level. Nomenclature: TPA₁-DOB₁-PMP₁-(CH₂)₈-PMP₂-DOB₂-TPA₂.

state	Fragment					
	TPA ₁	DOB ₁	PMP ₁	TPA ₂	DOB ₂	PMP ₂
S ₁	0.422	-0.394	-0.008	0.392	-0.476	0.065
S ₂	0.398	-0.469	0.071	0.418	-0.408	-0.009
S ₃	0.216	-0.256	0.012	0.038	-0.146	0.135
S ₄	0.032	-0.143	0.133	0.219	-0.257	0.013
S ₅	0.164	-0.168	0.078	0.007	-0.187	0.103
S ₆	0.003	-0.186	0.100	0.170	-0.164	0.077
S ₇	0.034	-0.360	0.335	0.014	-0.362	0.339
S ₈	0.011	-0.361	0.338	0.039	-0.360	0.333

Table S18: Mulliken analysis of the difference in charge in comparison to the ground state for the diabatic states of dimer **3'** (folded form) computed at the B3LYP/6-31+G(d) level. Nomenclature: (*m*Ph₁,PMP_{1a})-DOB₁-PMP_{1b}-(CH₂)₈-PMP_{2b}-DOB₂-(PMP_{2a},*m*Ph₂).

diabat	Fragment							
	<i>m</i> Ph ₁	PMP _{1a}	DOB ₁	PMP _{1b}	PMP _{2a}	DOB ₂	PMP _{2b}	<i>m</i> Ph ₂
<i>Z</i> ₁	-0.006	0.199	-0.193	0.005	0.005	-0.194	0.211	-0.070
<i>Z</i> ₂	0.001	0.152	-0.091	0.005	0.005	-0.163	0.089	0.001
<i>Z</i> ₃	0.002	0.090	-0.162	0.005	0.004	-0.090	0.149	0.001
<i>Z</i> ₄	0.001	0.078	-0.169	0.039	0.063	-0.111	0.096	0.002
<i>Z</i> ₅	0.002	0.005	-0.002	0.002	0.041	-0.379	0.042	0.287
<i>Z</i> ₆	0.291	0.041	-0.379	0.039	0.005	-0.004	0.003	0.002
<i>Z</i> ₇	0.111	0.053	-0.211	0.048	0.044	-0.210	0.051	0.113
<i>Z</i> ₈	0.109	0.049	-0.210	0.044	0.056	-0.207	0.050	0.111
<i>Z</i> ₉	0.113	0.045	-0.211	0.051	0.052	-0.210	0.051	0.109
<i>Z</i> ₁₀	0.107	0.052	-0.209	0.045	0.050	-0.210	0.053	0.112

8 Splitting of *S*₁ and *S*₂ in dimer **2'**

The evaluation of the (classical) dipole-dipole interaction (equation S.13) corresponding to the interaction between monomeric excitations in dimer **2'** has been done by considering the following parameters from *S*₁ transition in monomer **1** and the optimized V-shape structure of dimer **2'** in DCM solution at the B3LYP/6-31+G(d) computational level.

$$\Delta E = \frac{1}{4\pi\epsilon_0} \left[\frac{\mathbf{d}_1 \cdot \mathbf{d}_2}{|\mathbf{R}|^3} - 3 \frac{(\mathbf{R} \cdot \mathbf{d}_1)(\mathbf{R} \cdot \mathbf{d}_2)}{|\mathbf{R}|^5} \right] \quad (\text{S.13})$$

where \mathbf{d}_i are the transition dipole moments for the two monomers, \mathbf{R} is the distance between the two dipoles and ΔE is the energy shift of the excitation energies of the dimer with respect to the transition energy for the monomer. Data: $|\mathbf{d}_i| = 36.3865$ D; $|\mathbf{R}| = 18.52$ Å; $\theta_{12} = 65.36^\circ$; $\theta_{12} = 65.36^\circ$; $\theta_1 = 57.79^\circ$; $\theta_2 = 56.85^\circ$.

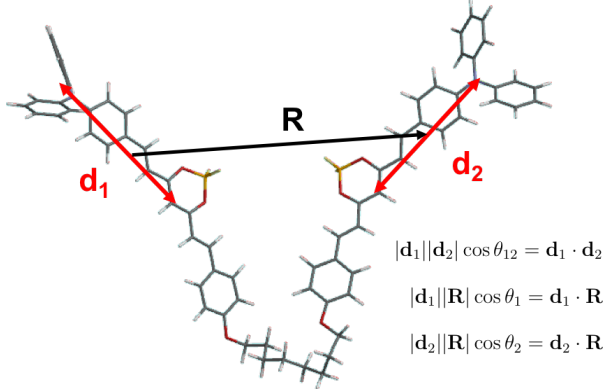


Figure S9: Dipole-dipole interaction representation for dimer **2'**.

The gap between the two lowest singlet states of the dimer, i.e. Davydson splitting, is obtained as the sum of the energy shifts corresponding to in-phase and out-of-phase combinations of the \mathbf{d}_1 and \mathbf{d}_2 dipoles and corresponds to $\Delta E_{Dav} = 2\Delta E = 0.11$ eV.

9 Dimer **2'**: CAM-B3LYP calculations

Electronic structure of low-lying states of curcumin dimers **1'** and **3'** obtained with hybrid GGA (B3LYP) and long-range corrected (CAM-B3LYP) functionals provide qualitatively the same transitions with excitation energies systematically larger for CAM-B3LYP. On the other hand, the nature of electronic transitions (beyond S_2 state) in **2'** present larger discrepancies between B3LYP and CAM-B3LYP due to the large interchromophoric separation in **2'** and the strong stabilization of inter-CT transitions by non LRC functionals, such as B3LYP. In the following we present additional calculations on the singlet excited states of dimer **2'**.

Table S19: Excitation energies (in eV) and oscillator strengths (in parenthesis) computed at the CAM-B3LYP/6-31+G(d) level within TDA in gas phase for the open form of **2'** dimer.

dimer	state	ΔE	strength
2' (V-shape)	S_1	3.73	1.965
	S_2	3.73	1.906
	S_3	4.00	0.898
	S_4	4.00	0.867
	S_5	4.34	0.006
	S_6	4.35	0.005
	S_7	4.45	0.015
	S_8	4.46	0.172

Table S20: Diabatic excitation energies (in eV) computed at the CAM-B3LYP/ 6-31+G* level (within TDA) in gas phase for the V-shaped form of **2'** dimer.

dimer	state	ΔE
2' (V-shape)	Z_1	3.73
	Z_2	3.73
	Z_3	3.99
	Z_4	4.00
	Z_5	4.32
	Z_6	4.34
	Z_7	4.45
	Z_8	4.45

Table S21: Mulliken analysis of the difference in charge in comparison to the ground state for the two diabatic states for the dimer **2'** (V-shape) computed at the CAM-B3LYP/6-31+G(d) level. Nomenclature: TPA₁-DOB₁-PMP₁-(CH₂)₈-PMP₂-DOB₂-TPA₂.

diabat	Fragment					
	TPA ₁	DOB ₁	PMP ₁	TPA ₂	DOB ₂	PMP ₂
Z_1, Z_2	0.430	-0.420	-0.010	0.430	-0.420	-0.010
Z_3, Z_4	0.030	-0.370	0.335	0.030	-0.370	0.335
Z_5	0.000	-0.080	0.210	0.000	-0.150	0.020
Z_6	0.000	-0.150	0.020	-0.005	-0.080	0.210
Z_7	0.150	-0.050	0.015	0.000	-0.120	0.005
Z_8	0.000	-0.120	0.005	0.150	-0.050	0.015

References

- (1) Narasimha, K.; Jayakannan, M. π -Conjugated Polymer Anisotropic Organogel Nanofibrous Assemblies for Thermoresponsive Photonic Switches. *ACS Appl. Mater. Interfaces* **2014**, *6*, 19385–19396.
- (2) Reutov, V. A.; Gukhman, E. V.; Kafitulova, E. E. Boron Difluoride β -Diketonates: III. Boron Difluoride 3-Organypenta-2,4-dionates. *Russ. J. Gen. Chem.* **2003**, *73*, 1441–1444.

(3) Fraser, C. L.; Zhang, G. Mechanochromic luminescent difluoroboron beta-diketonates. US 9074129B2, 2015.